

# Angularity event shapes for DIS in Soft-Collinear Effective Field theory (SCET)

Tanmay Maji



NIT Kurukshetra

19 Dec. 2022

QEIC2022 IIT Delhi

Coauthors: Jiawei Zhu, Daekyoung Kang, Fudan University, Shanghai

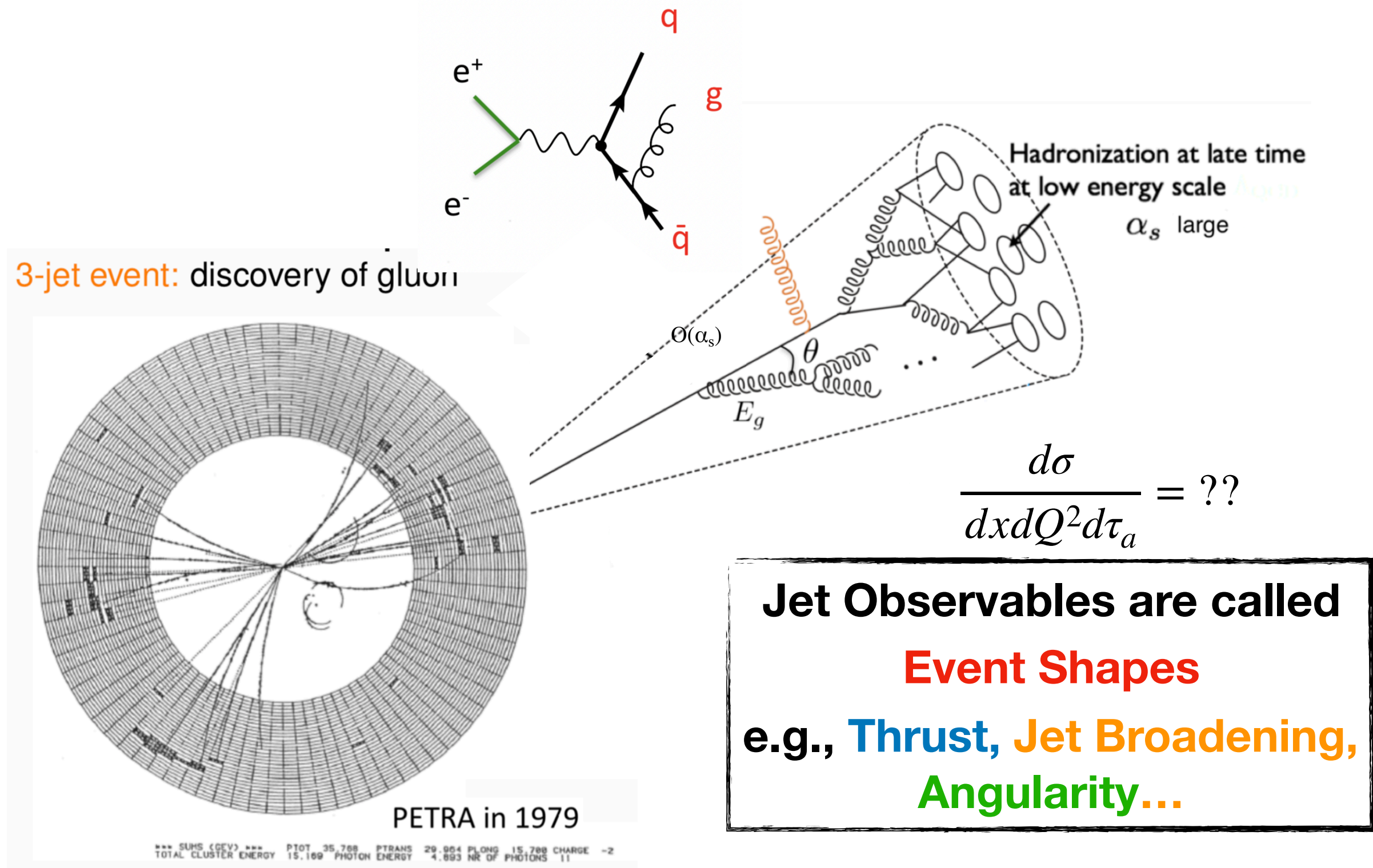
# Talk organized as...

---

- Introduction
- Jet Event Shapes and angularity
- Event Shapes in DIS
- Angularity beam functions at next-to-next-to-leading log (NNLL)
- Angularity differential cross-section at NNLL
- Prediction & Remarks for future EIC

# Jets and Jet Event Shapes?

- In high energy scattering, the most common final states are collimated branches of strongly interacting particles, called jet.



## Thrust: Characterizes the geometry of collision

---

$$\tau = \frac{2}{Q} \sum_{i \in \mathcal{X}} |\mathbf{p}_\perp^i| e^{-|\eta_i|}$$

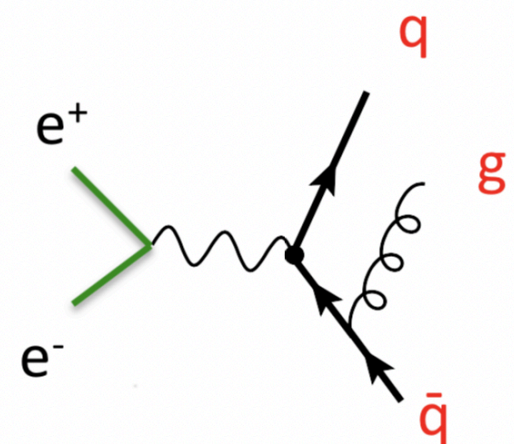
$$\text{Rapidity: } \eta = \frac{1}{2} \ln \left( \frac{p^-}{p^+} \right)$$

## Thrust: Characterizes the geometry of collision

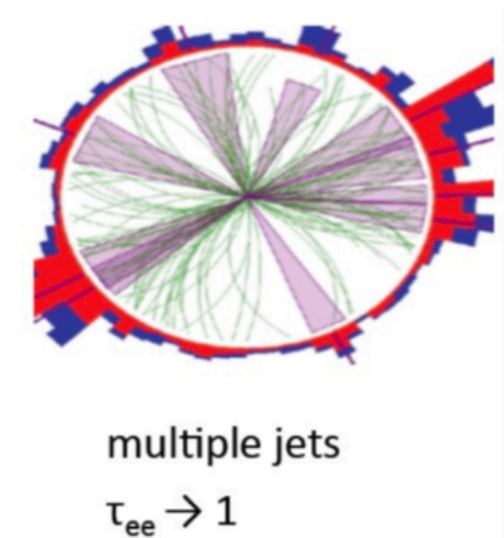
$$\tau = \frac{2}{Q} \sum_{i \in \chi} |\mathbf{p}_\perp^i| e^{-|\eta_i|}$$

Rapidity:  $\eta = \frac{1}{2} \ln \left( \frac{p^-}{p^+} \right)$

An example:



$$\begin{aligned} n &= (1, 0, 0, 1) \\ \bar{n} &= (1, 0, 0, -1) \end{aligned}$$



$$= \frac{2}{Q^2} \sum_{i \in \chi} \min\{p_i \cdot n, p_i \cdot \bar{n}\}$$

# Angularity Event Shapes

—C. F. Berger, T. Kucs and G. F. Sterman' 200

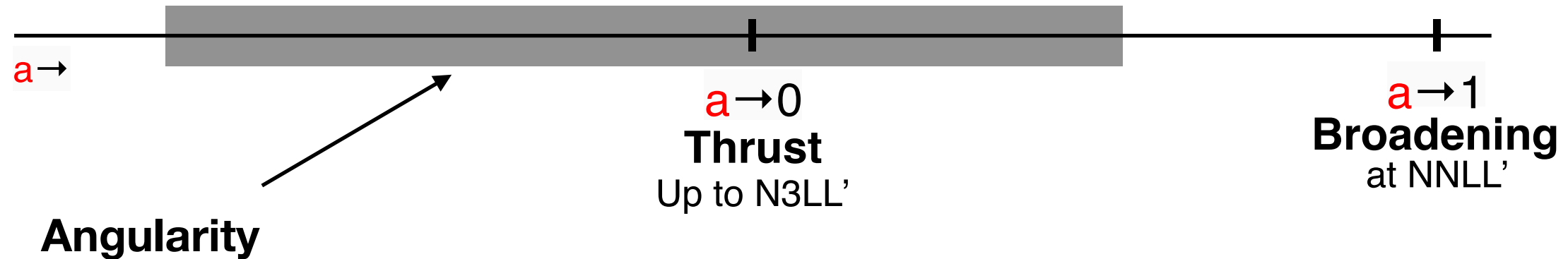
$$\tau_a = \frac{2}{Q} \sum_{i \in \mathcal{X}} |\mathbf{p}_\perp^i| e^{-|\eta_i|(1-a)}$$

Depends on  
continuous  
parameter

$$\eta = \frac{1}{2} \ln \left( \frac{p^-}{p^+} \right)$$

A more general event shape!

provide access from thrust to jet broadening in continuous manner



# Angularity Event Shapes

—C. F. Berger, T. Kucs and G. F. Sterman' 200

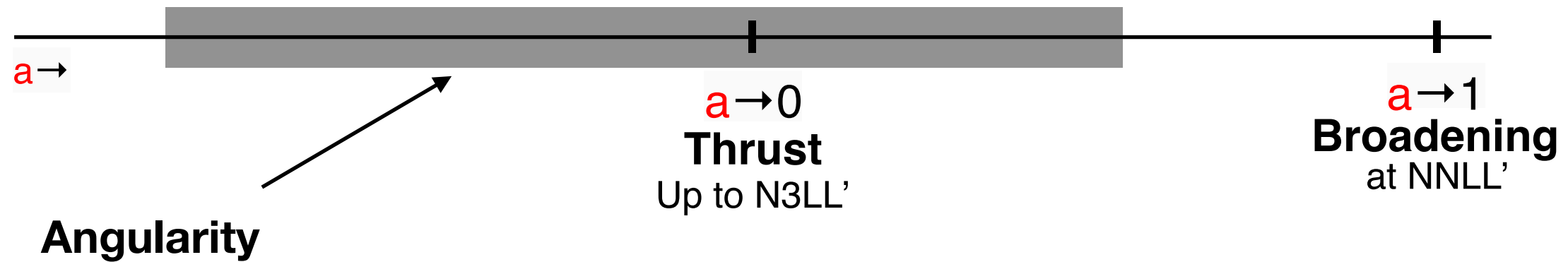
$$\tau_a = \frac{2}{Q} \sum_{i \in \chi} |\mathbf{p}_\perp^i| e^{-|\eta_i|(1-a)}$$

Depends on continuous parameter

$$\eta = \frac{1}{2} \ln \left( \frac{p^-}{p^+} \right)$$

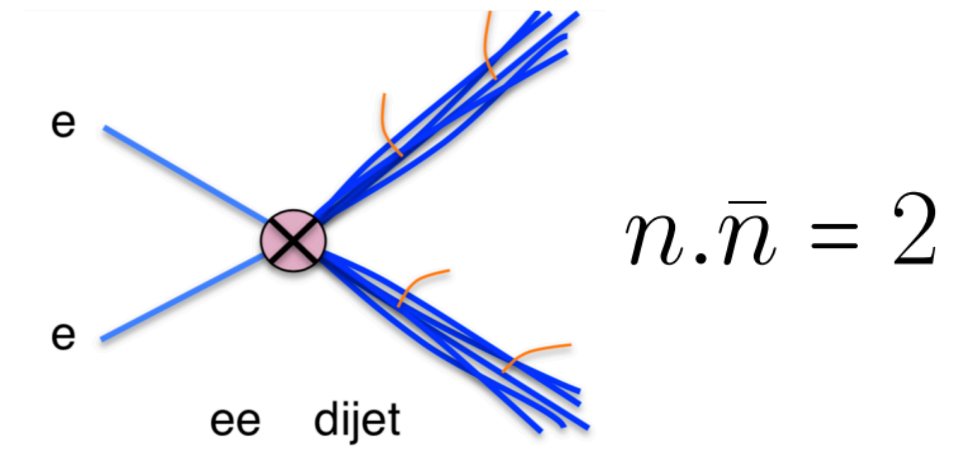
A more general event shape!

provide access from thrust to jet broadening in continuous manner

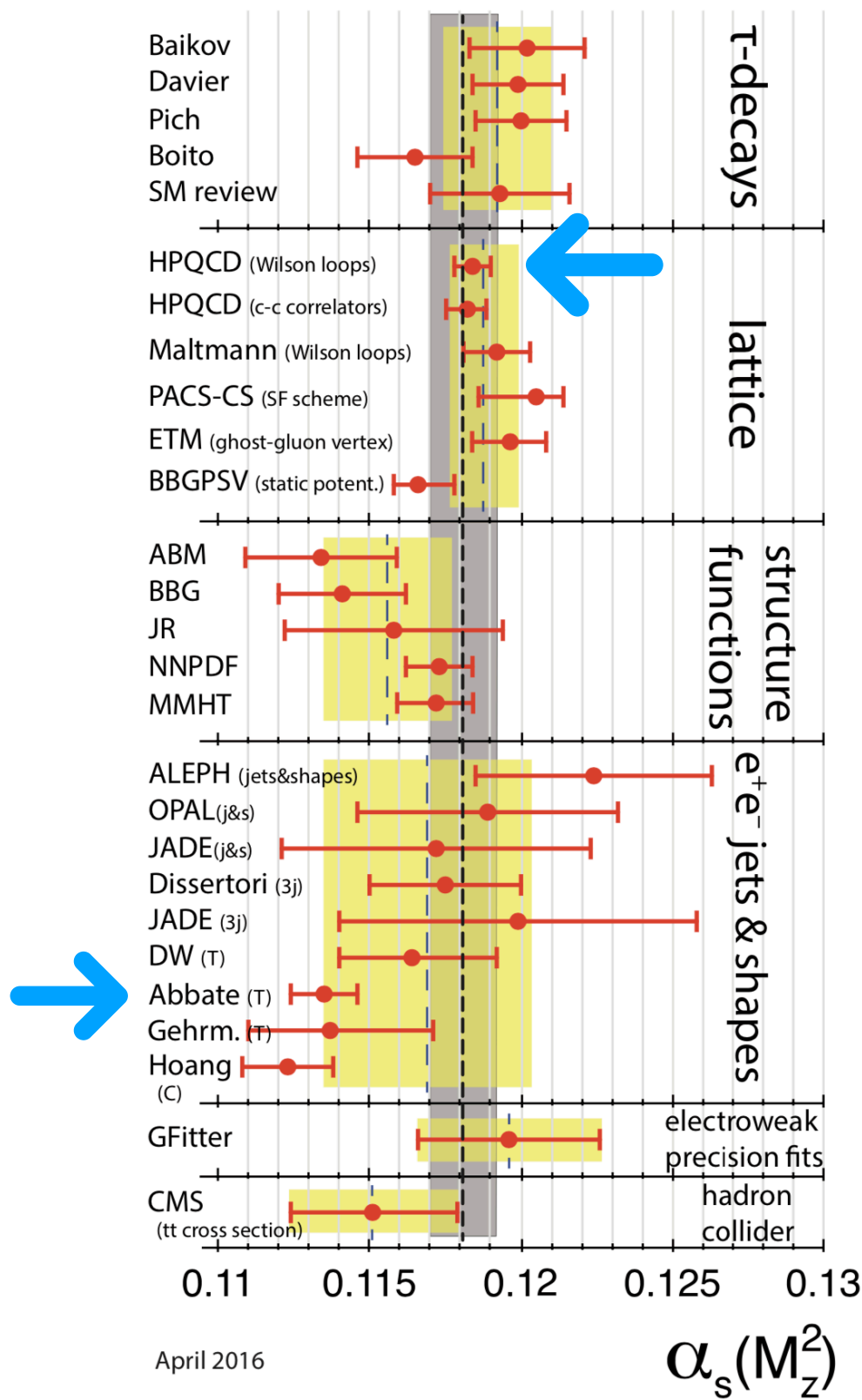


For  $e^+e^- = \text{dijet}$

$$\tau_a^{ee} = \frac{2}{Q^2} \sum_{i \in \chi} \min \left\{ (p_i \cdot n)^{a/2} (p_i \cdot \bar{n})^{(1-a)/2} \right\}$$

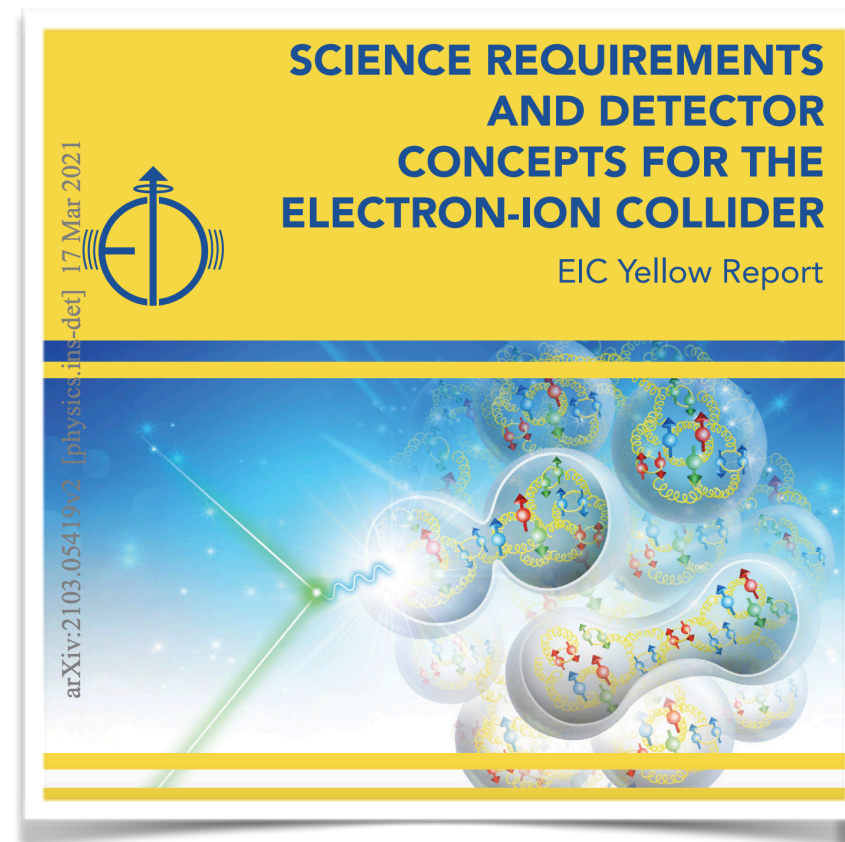


# Why DIS angularity? Puzzle in Strong Coupling determination



# Why DIS angularity?

- Shed lights on the puzzle in strong coupling constant determination
- DIS event shapes for future **Electron-Ion-Collider (EIC)** at BNL!!



process, although acceptance up to higher rapidity (for example,  $\eta = 4.5$ ) would provide a longer lever arm allowing for more stringent tests of the small- $x$  dynamics and the Pomeron. Apart from  $J/\psi$  production, the rapidity-gap production of  $\rho$ -mesons maybe also very promising, perhaps even over a broader  $|t|$ -range.

## 7.1.7 Global event shapes and the strong coupling constant

### Introduction

Event shapes [289] are global measures of the momentum distribution of hadrons in the final state of a collision, using a single number to characterize how well collimated the hadrons are along certain axes. This simple and global nature makes them highly amenable to high-precision theoretical calculations and convenient for experimental measurements. They then become powerful probes of QCD predictions, the strong coupling  $\alpha_s$ , hadronization effects, etc.

The classic example, for collisions  $e^+e^- \rightarrow X$ , is *thrust* [290,291],

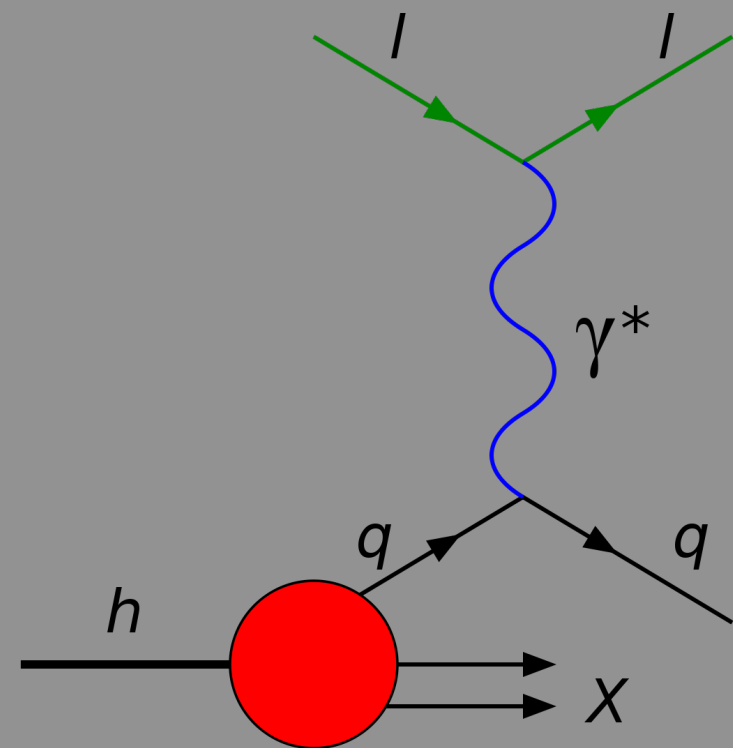
$$\tau = 1 - T, \quad \text{where} \quad T = \frac{1}{Q} \max_{\hat{t}} \sum_{i \in X} |\hat{t} \cdot p_i| = \frac{2}{Q} p_z^A, \quad (7.13)$$

at a center-of-mass collision energy  $Q$ , summing the three-momenta  $p_i$  of all final-state hadrons  $i \in X$  projected onto the thrust axis  $\hat{t}$ , which is defined as the axis maximizing the sum. It is customary to use  $\tau = 1 - T$ , whose  $\tau \rightarrow 0$  limit describes pencil-like back-to-back two-jet events, and which grows as the jets broaden, up to the limit  $\tau = 1/2$  for a spherically symmetric final state. Other examples of two-jet event shapes in  $e^+e^-$  are broadening  $B$  [292],  $C$ -parameter [293], and angularities [294,295].

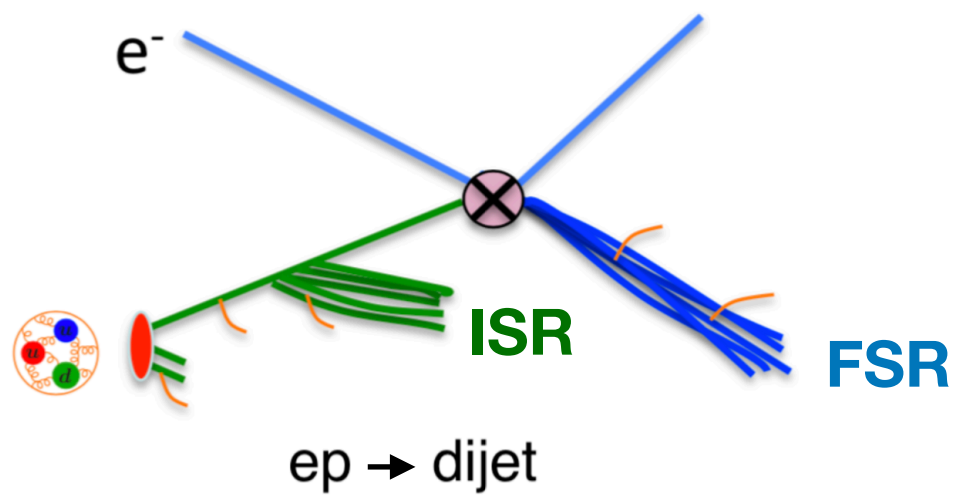
Could be an early milestone!

# Angularity in the deep-inelastic scattering!

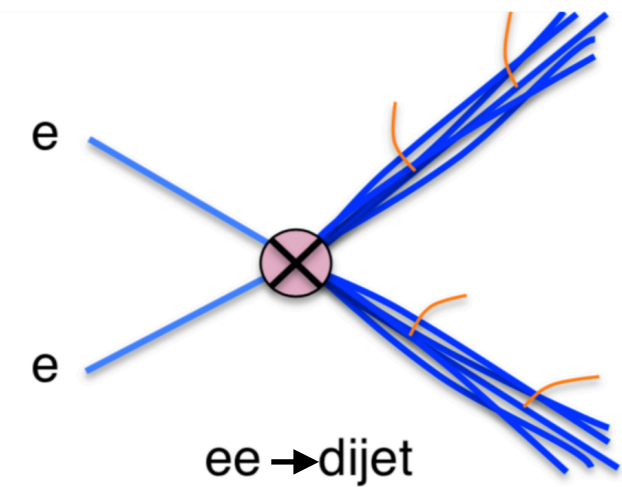
$$e(l) + N(P) \rightarrow e(l') + \text{dijet}$$



# Angularity for DIS



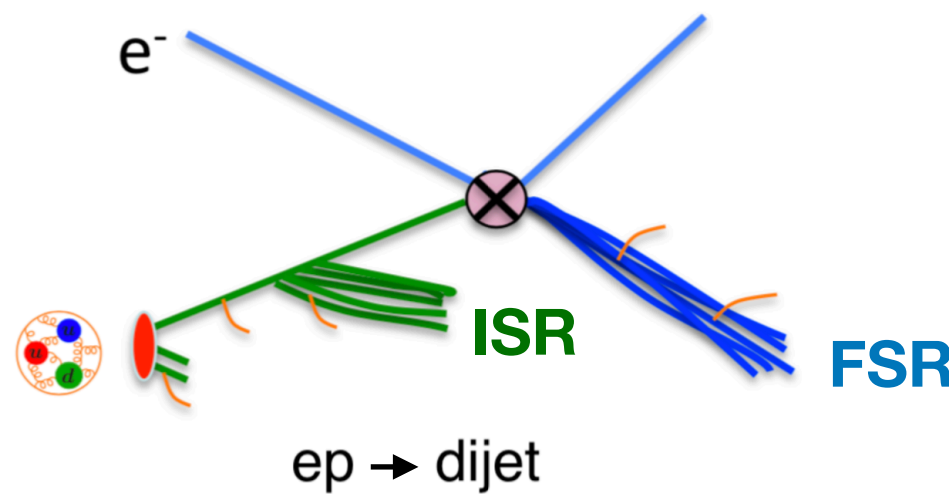
Not back to back even in CM !!



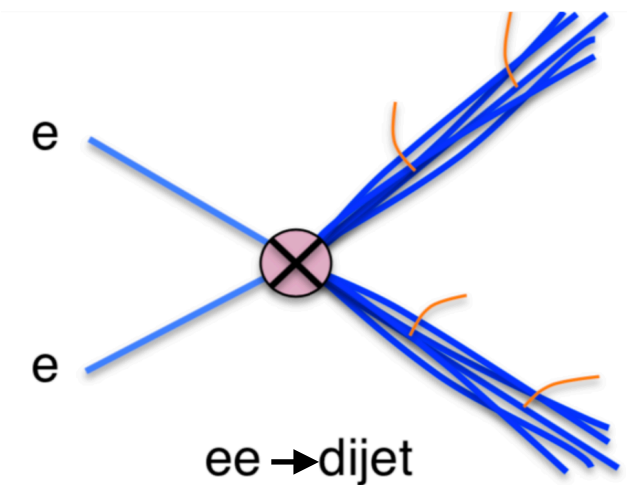
Back to back in CM frame

$$n.\bar{n} = 2$$

# Angularity for DIS



Not back to back even in CM !!



Back to back in CM frame

$$n_i \cdot \bar{n}_i = 2$$

**Axis Choice:**  $qB = xP$ ,  $qJ = \text{jet axis}$

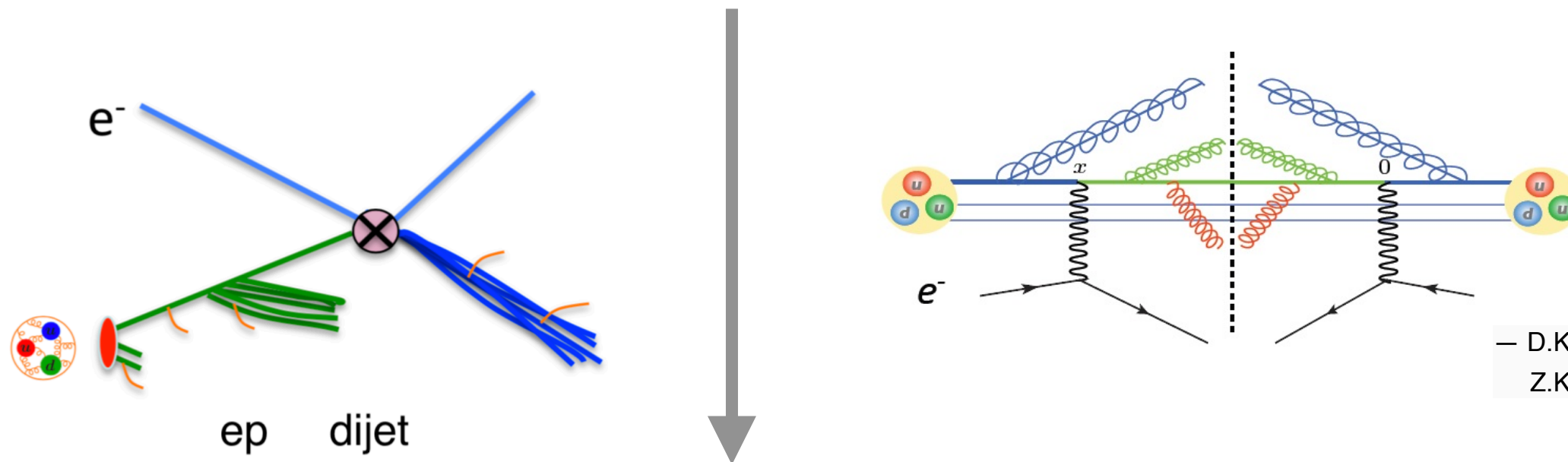
$$q_B^\mu = \omega_B \frac{n_B^\mu}{2} \quad \text{and} \quad q_J^\mu = \omega_J \frac{n_J^\mu}{2} \quad \text{with} \quad n_i \cdot \bar{n}_i = 2$$

we obtain  $\omega_B = \bar{n}_B \cdot q_B$  and  $\omega_J = \bar{n}_J \cdot q_J$

$$\tau_a = \frac{2}{Q^2} \sum_{i \in \mathcal{X}} \min \left\{ (q_B \cdot p_i) \left( \frac{q_B \cdot p_i}{q_J \cdot p_i} \right)^{-a/2}, (q_J \cdot p_i) \left( \frac{q_J \cdot p_i}{q_B \cdot p_i} \right)^{-a/2} \right\}$$

# Angularity diff. cross-section for DIS

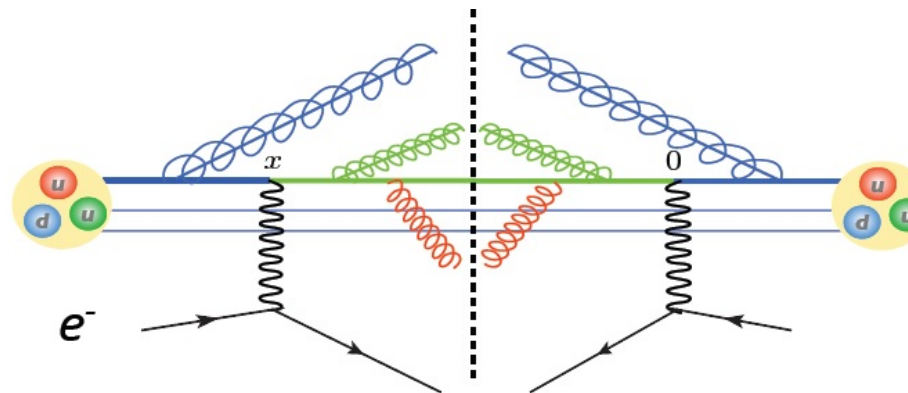
$$\frac{d\sigma}{dx dQ^2 d\tau_a} = L_{\mu\nu}(x, Q^2) W^{\mu\nu}(x, Q^2, \tau_a)$$



— D.Kang,Lee,Stewart'2013  
Z.Kang,Mantry,Qiu'2012

$$\frac{d\sigma}{dx dQ^2 d\tau_a} = \frac{d\sigma_0}{dx dQ^2} \int d\tau_a^J d\tau_a^B d\tau_a^S \delta(\tau_a - \tau_a^J - \tau_a^B - \tau_a^S) \times \sum_{i=q,\bar{q}} H_i(Q^2, \mu) \mathcal{B}_i(\tau_a^B, x, \mu) J(\tau_a^J, \mu) S(\tau_a^S, \mu)$$

# Power counting in SCET



$$p = p^+ \frac{\bar{n}_B}{2} + p^- \frac{n_B}{2} + p_\perp$$

**Collinear and soft modes**

$$\begin{aligned} p_c &\sim Q(\lambda_c^2, 1, \lambda_c), & \tau_a^B(p_c) &\sim \lambda_c^{2-a} \\ p_s &\sim Q(\lambda_s, \lambda_s, \lambda_s), & \tau_a^B(p_s) &\sim \lambda_s \end{aligned}$$

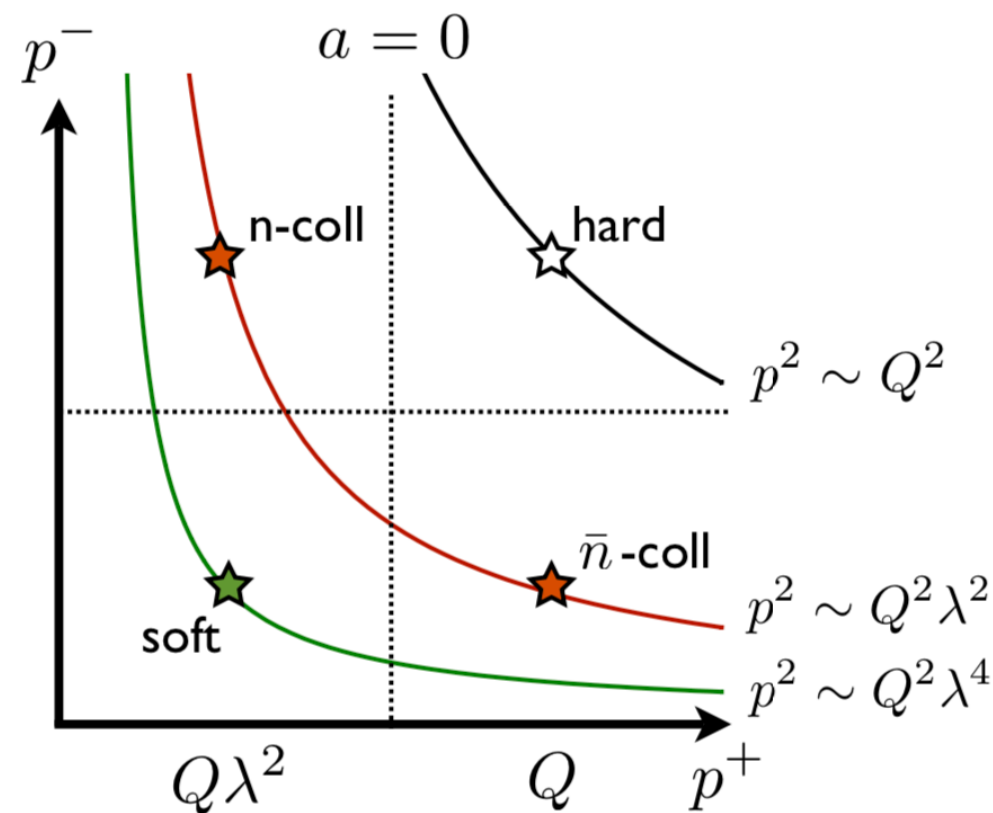
This implies relevant soft mode contributing to  $\tau_a^B$  has a scale of

$$\lambda_s \sim \lambda_c^{2-a}.$$

# Soft and collinear splitting

$$p_c^2 \sim Q^2 \lambda^{2-a} \quad p_s^2 \sim Q^2 \lambda^{2(2-a)}$$

$$\begin{aligned} p_\perp = 0 & \text{ plane} \\ p^2 = p^+ p^- \end{aligned}$$



**SCET facto.:**  $d\sigma = \text{Hard} \times \text{Beam} \otimes \text{Jet} \otimes \text{Soft}$

# Soft and collinear splitting

$$\frac{d\sigma}{dxdQ^2d\tau_a} = \frac{d\sigma_0}{dxdQ^2} \int d\tau_a^J d\tau_a^B d\tau_a^S \delta(\tau_a - \tau_a^J - \tau_a^B - \tau_a^S) \times \sum_{i=q,\bar{q}} H_i(Q^2, \mu) \mathcal{B}_i(\tau_a^B, x, \mu) J(\tau_a^J, \mu) S(\tau_a^S, \mu)$$

—Hornig, Lee, Ovanesyan'09;  
—Bell, Hornig, Lee, Talbert'18,

**Beam func.:**  $B(\tau_a, x, \mu) = \begin{matrix} \text{pdf} \otimes [\delta_{qj} \delta(\tau_a) + \tilde{\mathcal{I}}_{qj}^{(1)} + \mathcal{O}(\alpha_s^2) + \dots] \\ NP \quad LO \quad NLO \quad NNLO \end{matrix}$

The angularity Bean function is presented for the first time

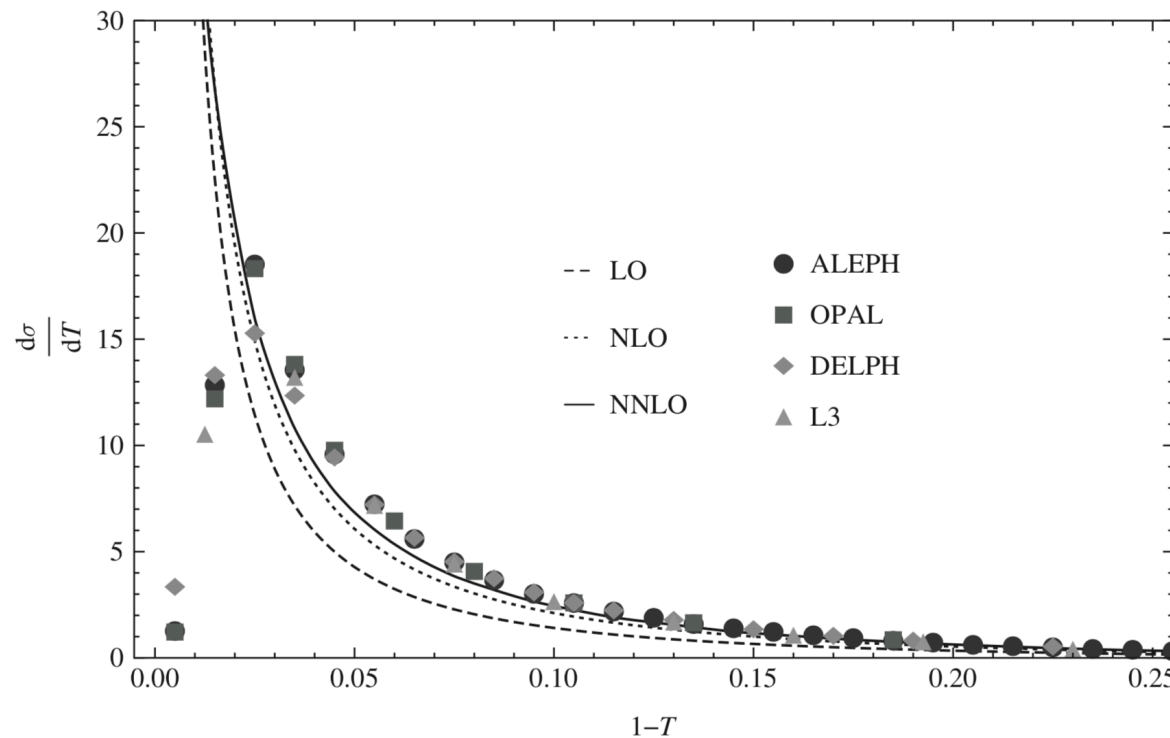
— Tanmay Maji, D. Kang, J. Zhu, JHEP11(2021) 026

# Large logs at threshold limit & Resummation

$$G^{\text{fixed}}(L_G, \mu) = 1 + \frac{\alpha_s(\mu)}{4\pi} \left[ -j_G \kappa_G \frac{\Gamma_0}{2} L_G^2 - \gamma_0^G L_G + c_1^G \right], \quad G = \{H, \tilde{S}, \tilde{J}\}$$

$$L_B(\tau_a) = \log\left[\frac{Q}{\mu_B}(\tau_a e^{-\gamma_E})^{1/j_B}\right]$$

With  $j_B = 2-\alpha$



$\sigma = \sigma^{(0)}$  leading order (**LO**)

$+ \alpha_s \sigma^{(1)}$  next-to-leading order (**NLO**)

$+ \alpha_s^2 \sigma^{(2)}$  next-next-to-leading order (**NNLO**)

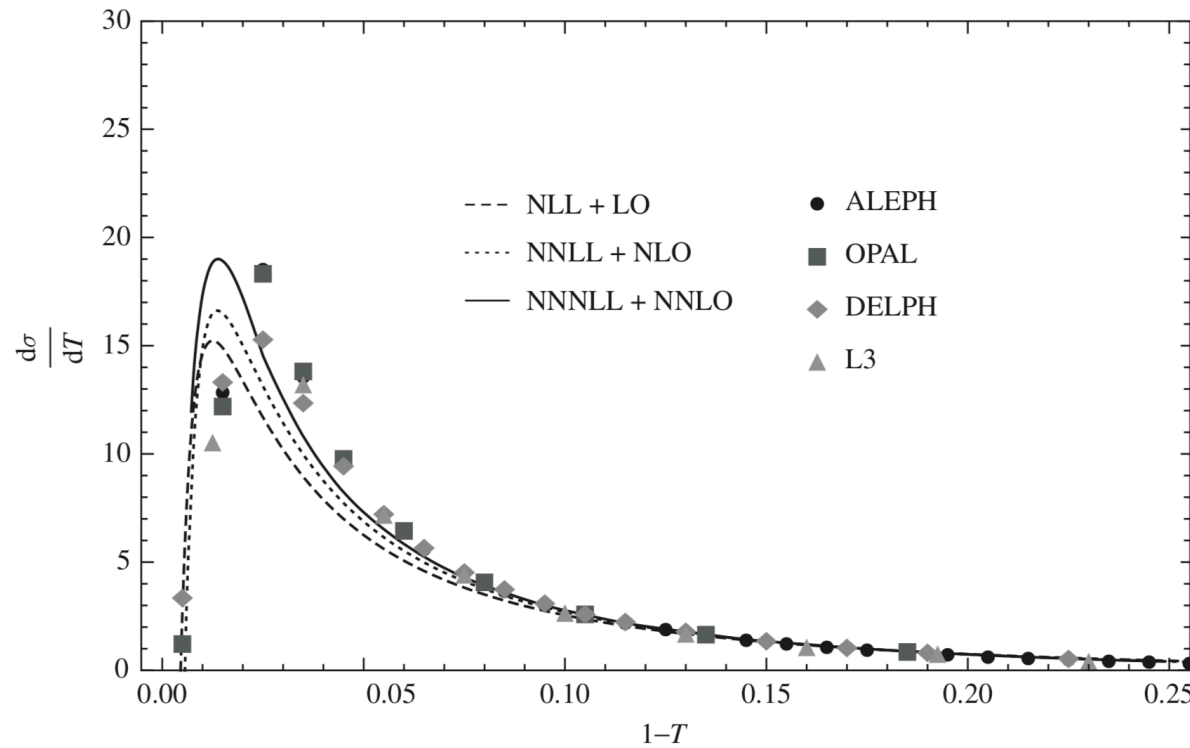
$+ \dots$

# Large logs at threshold limit & Resummation

$$G^{\text{fixed}}(L_G, \mu) = 1 + \frac{\alpha_s(\mu)}{4\pi} \left[ -j_G \kappa_G \frac{\Gamma_0}{2} L_G^2 - \gamma_0^G L_G + c_1^G \right], \quad G = \{H, \tilde{S}, \tilde{J}\}$$

$$L_B(\tau_a) = \log \left[ \frac{Q}{\mu_B} (\tau_a e^{-\gamma_E})^{1/j_B} \right]$$

With  $j_B = 2-\alpha$



$$\sigma = \sigma^{(0)}$$

leading order (**LO**)

$$+ \alpha_s \sigma^{(1)}$$

next-to-leading order (**NLO**)

$$+ \alpha_s^2 \sigma^{(2)}$$

next-next-to-leading order (**NNLO**)

$$+ \dots$$

$$K_B(\mu_B, \mu) = L_B \sum_{k=1}^{\infty} (\alpha_s L_B)^k$$

Leading Log (**LL**)

$$+ \sum_{k=1}^{\infty} (\alpha_s L_B)^k$$

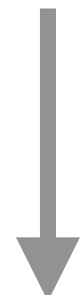
Next-to-leading Log (**NLL**)

$$+ \dots$$

Next-to-next-leading Log (**NNLL**)

## Resummation in Laplace space

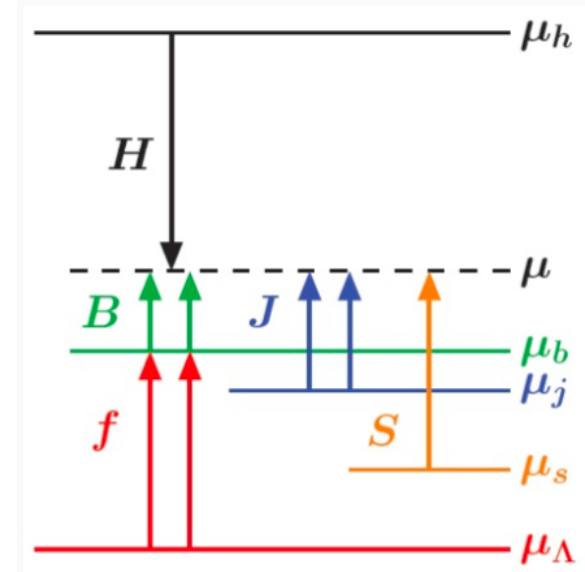
$$\begin{aligned}\frac{d\sigma}{dxdQ^2d\tau_a} &= \frac{d\sigma_0}{dxdQ^2} \int d\tau_a^J d\tau_a^B d\tau_a^S \delta(\tau_a - \tau_a^J - \tau_a^B - \tau_a^S) \\ &\times \sum_{i=q,\bar{q}} H_i(Q^2, \mu) \mathcal{B}_i(\tau_a^B, x, \mu) J(\tau_a^J, \mu) S(\tau_a^S, \mu)\end{aligned}$$



$$G(\nu, \mu) = \int_0^\infty d\tau_a e^{-\nu\tau_a} G(\tau_a, \mu)$$

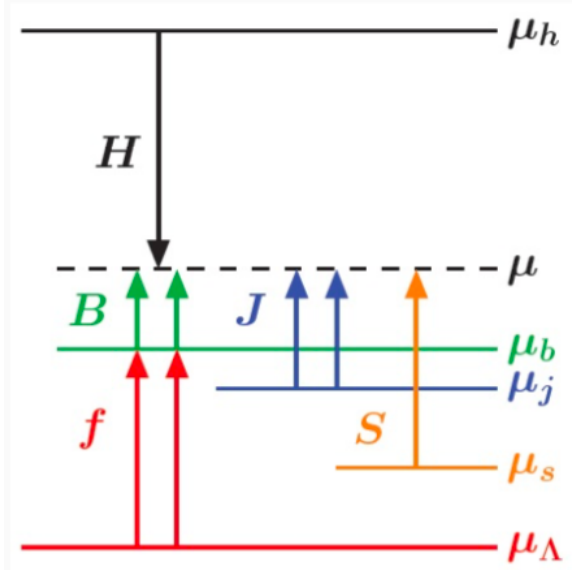
$$\tilde{\sigma}_q(\nu) = H_q(Q^2, \mu) \mathcal{B}_q(\nu, \mu) \tilde{J}(\nu, \mu) \tilde{S}(\nu, \mu)$$

# Resummation of large logs



$$\mu_H = Q, \quad \mu_{J,B} = Q\tau_a^{1/(\bar{2}-a)}, \quad \mu_S = Q\tau_a$$

# Resummation of large logs



$$\mu_H = Q, \quad \mu_{J,B} = Q\tau_a^{1/(\bar{2}-a)}, \quad \mu_S = Q\tau_a$$

Evolution Equation for beam function

$$\mu \frac{d}{d\mu} B(\nu, \mu) = \gamma_G(\mu) B(\nu, \mu) ; \quad \text{similar to } J, S, H$$

Solution :  $B(\nu, \mu) = B(\nu, \mu_B) e^{K_B(\mu_B, \mu) + j_B \eta_B(\mu_B, \mu) L_B}$ ,

- Jet and beam functions are defined by same collinear operator:  $\gamma_J(\mu) = \gamma_B(\mu)$

$$K_B(\mu_B, \mu) = L_B \sum_{k=1}^{\infty} (\alpha_s L_B)^k + \sum_{k=1}^{\infty} (\alpha_s L_B)^k + \dots$$

*LL*

*NLL*

$$L_B = \ln(\mu/\mu_B)$$

$\alpha_s L_B \sim 1$

LL: Leading Log;  
NLL: Next-to-Leading Log

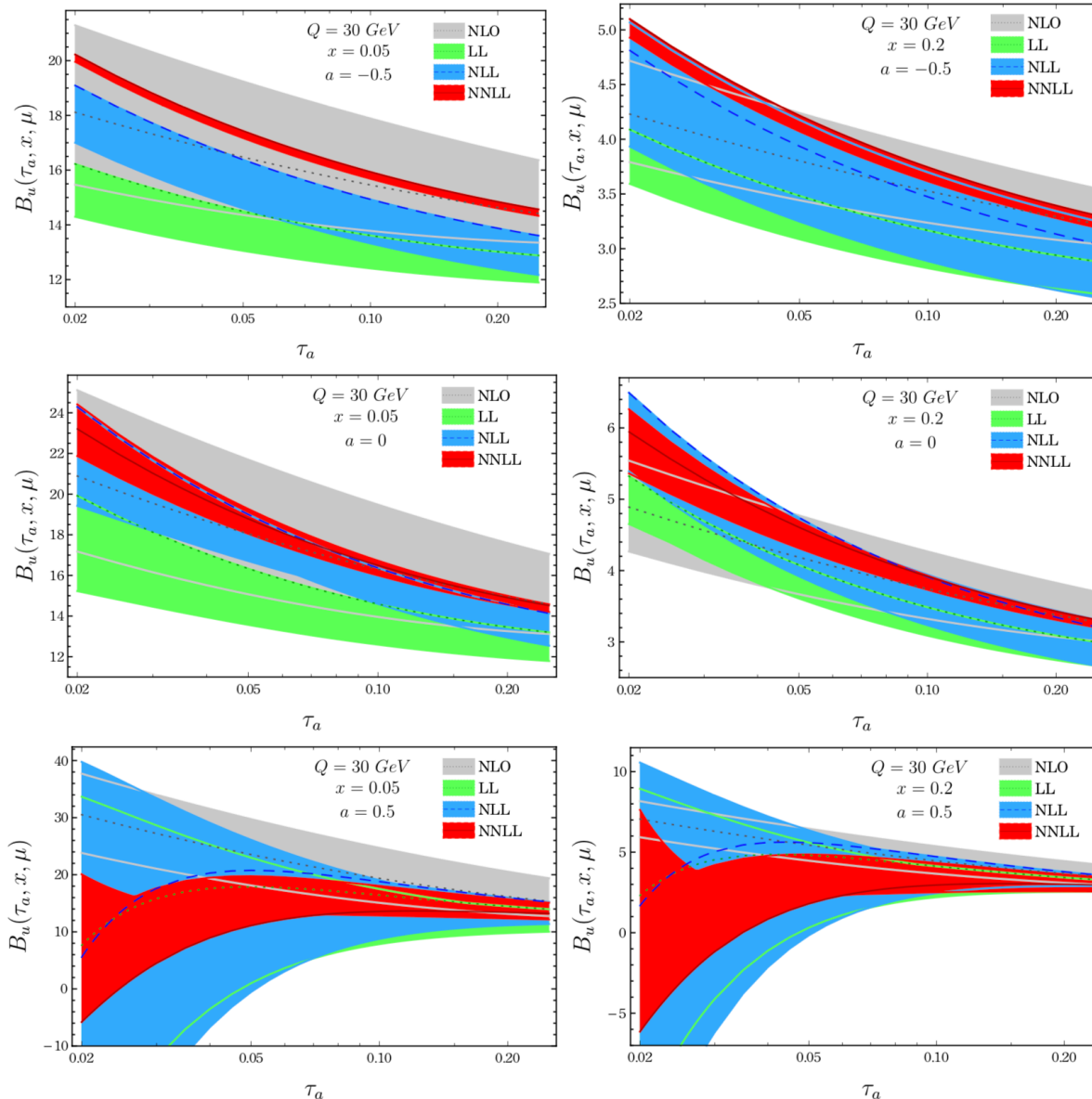
Results:  
Angularity Beam function

$$B(\tau_a^B, x, \mu)$$

# Angularity Beam function at NNLL accuracy

**Beam func.:**  $B(\tau_a, x, \mu) = \text{pdf} \otimes [\delta_{qj}\delta(\tau_a) + \tilde{\mathcal{I}}_{qj}^{(1)} + \mathcal{O}(\alpha_s^2) + \dots]$

NP	LO	NLO	NNLO
----	----	-----	------



$\wedge - a = -0.5$

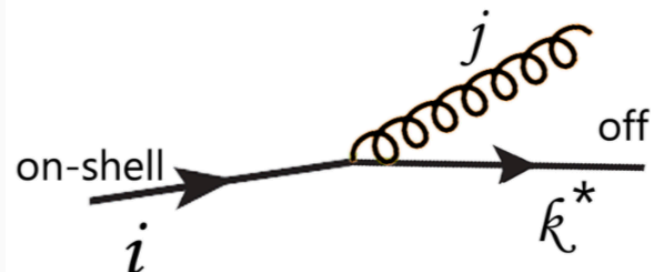
$\wedge - \text{Thrust limit}$

$\wedge - a = 0.5$

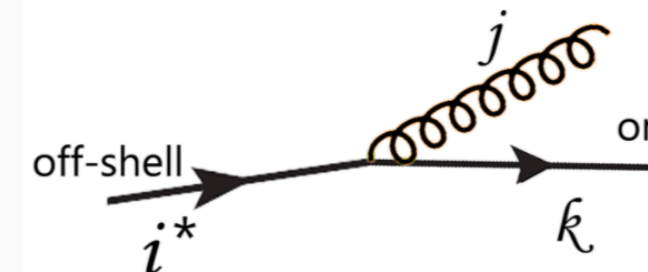
Resummation of large logs provides better perturbative convergence.

# Beam Func. & Fragmentation func.

Beam at NLO:  $i \rightarrow k^* j$



Fragmentation at NLO:  $i^* \rightarrow k j$



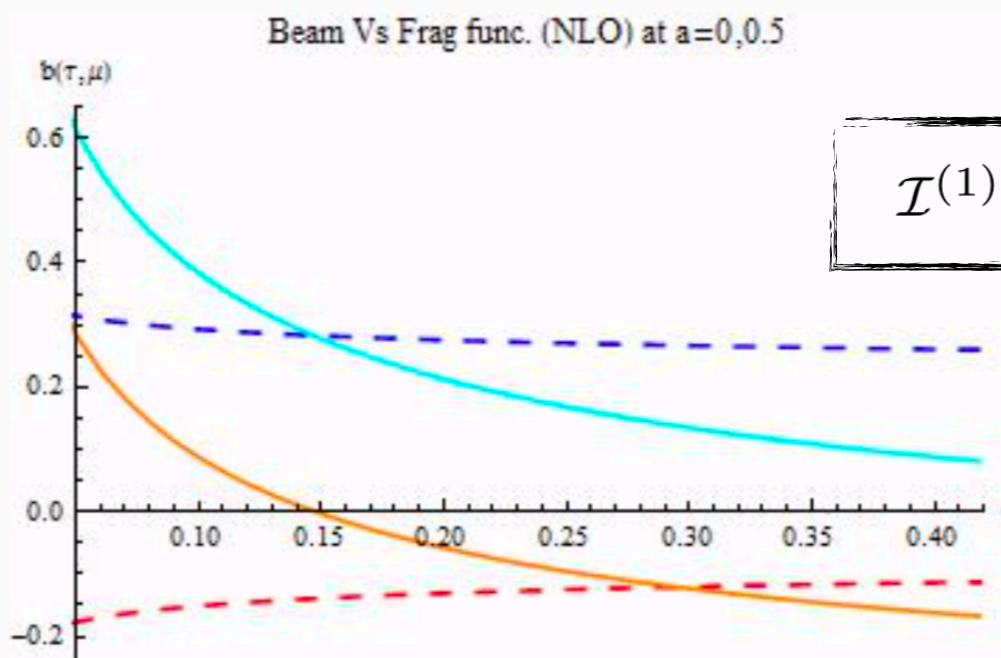
Crossing Symmetry!

Splitting Function:

[M.Ritzmann,W.J.Waalewijn,PRD90(2014)]

$$P_{i \rightarrow k^* j}(2pi.pj, x) \equiv (-1)^{\Delta_f} P_{k^* \rightarrow ij}(-2pi.pj, 1/x)$$

- Change comes only from the two-particle phase-space and effectively change in sign of the  $\log(x)$  term in the matching co-efficient  $\mathcal{I}^{(1)}$ .



$$\mathcal{I}^{(1)} \sim \dots - \frac{\alpha_s C_F}{2\pi} \frac{2(1-a)}{2-a} \frac{1+x^2}{1-x} \log x$$

Beam match. Coeff.:  $a = 0$

Beam match. Coeff.:  $a = 0.5$

FF match. Coeff.:  $a = 0$

FF match. Coeff.:  $a = 0.5$

- Difference decreases with the increase of angularity parameter  $a$ .

# Results

## Angularity Differential Cross-section

$$\frac{d\sigma^{DIS}}{dx dQ^2 d\tau_a} = ?$$

## Angularity Differential Cross-section

$$\frac{d\sigma}{dx dQ^2 d\tau_a} = \frac{d\sigma_0}{dx dQ^2} \sum_v H_v(Q^2, \mu) \int d\tau_a^J d\tau_a^B dk_S J_q(\tau_a^J, \mu) B_{v/q}(\tau_a^B, x, \mu) \\ \times S(k_S, \mu) \delta\left(\tau_a - \tau_a^J - \tau_a^B - \frac{k_S}{Q_R}\right),$$

# Angularity Differential Cross-section

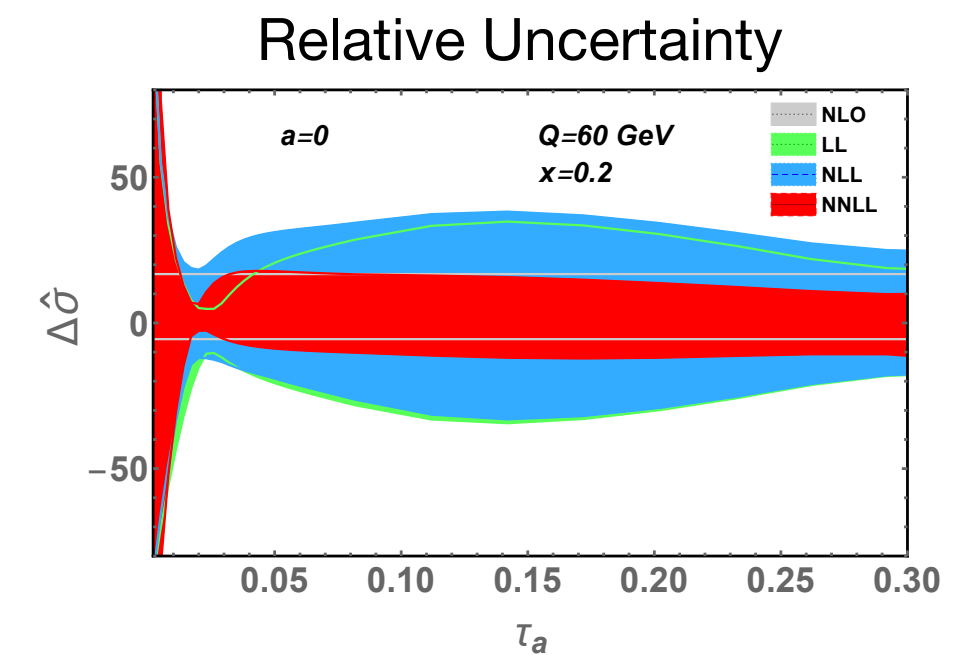
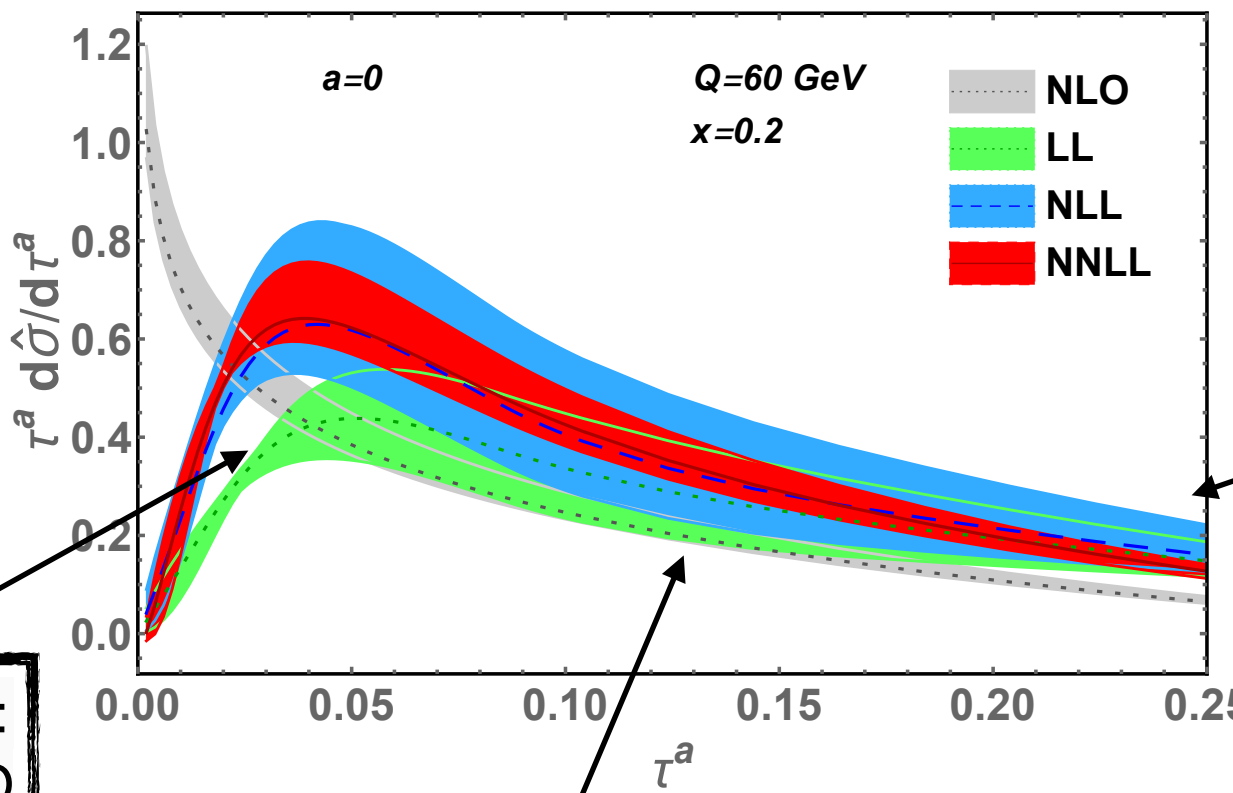
$$\frac{d\sigma}{dx dQ^2 d\tau_a} = \frac{d\sigma_0}{dx dQ^2} \sum_v H_v(Q^2, \mu) \int d\tau_a^J d\tau_a^B dk_S J_q(\tau_a^J, \mu) B_{v/q}(\tau_a^B, x, \mu) \\ \times S(k_S, \mu) \delta\left(\tau_a - \tau_a^J - \tau_a^B - \frac{k_S}{Q_R}\right),$$

Resummed result

$$\sigma(x, Q^2, \tau_a, \mu) = \sigma_0(x, Q^2) \left(\frac{Q}{\mu_H}\right)^{\eta_H(\mu, \mu_H)} e^{\kappa(\mu_H, \mu_J, \mu_B, \mu_S, \mu)} \\ \times \left(\left(\frac{Q}{\mu_J}\right)^{2-a} \tau_a e^{-\gamma_E}\right)^{\eta_J(\mu, \mu_J)} \left(\left(\frac{Q}{\mu_B}\right)^{2-a} \tau_a e^{-\gamma_E}\right)^{\eta_B(\mu, \mu_B)} \left(\frac{Q^2}{\mu_S} \tau_a e^{-\gamma_E}\right)^{2\eta_S(\mu, \mu_S)} \\ \times \tilde{j}_q \left( \partial_\Omega + \log\left(\frac{Q^{2-a}}{\mu_J^{2-a}} \tau_a e^{-\gamma_E}\right), \mu_J \right) \tilde{s} \left( \frac{1}{Q_R} \left( \partial_\Omega + \log\left(\frac{Q}{\mu_S} \tau_a e^{-\gamma_E}\right) \right), \mu_S \right) \\ \times \left[ H_q(y, Q^2, \mu_H) \tilde{b}_q \left( \partial_\Omega + \log\left(\frac{Q^{2-a}}{\mu_B^{2-a}} \tau_a e^{-\gamma_E}\right), x, \mu_B \right) \right. \\ \left. + H_{\bar{q}}(y, Q^2, \mu_H) \tilde{b}_{\bar{q}} \left( \partial_\Omega + \log\left(\frac{Q^{2-a}}{\mu_B^{2-a}} \tau_a e^{-\gamma_E}\right), x, \mu_B \right) \right] \frac{1}{\tau_a \Gamma(\Omega)}$$

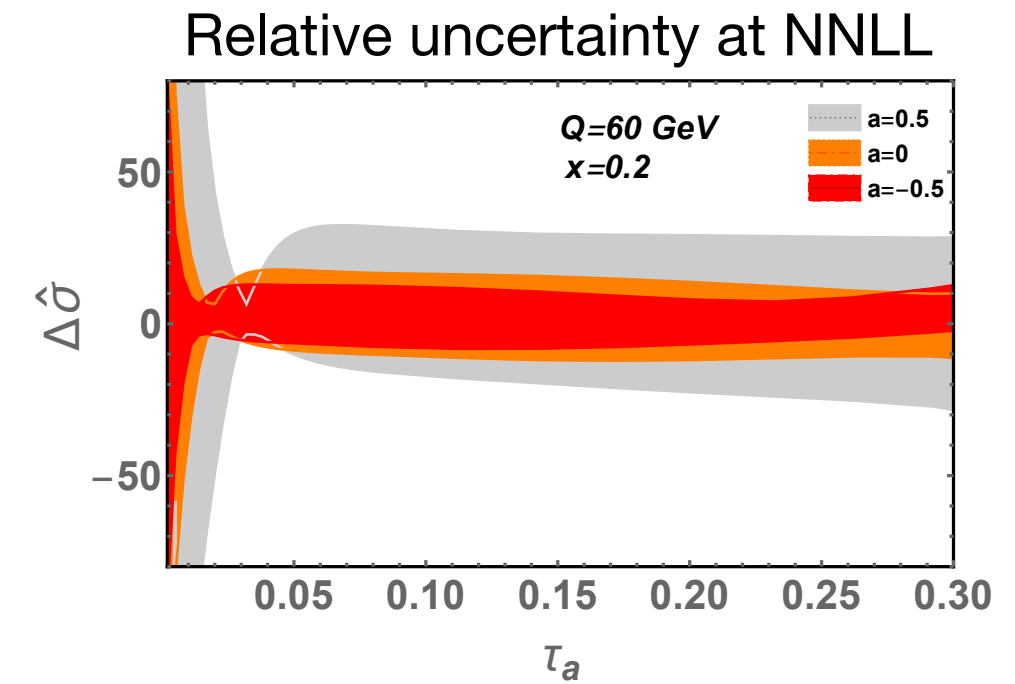
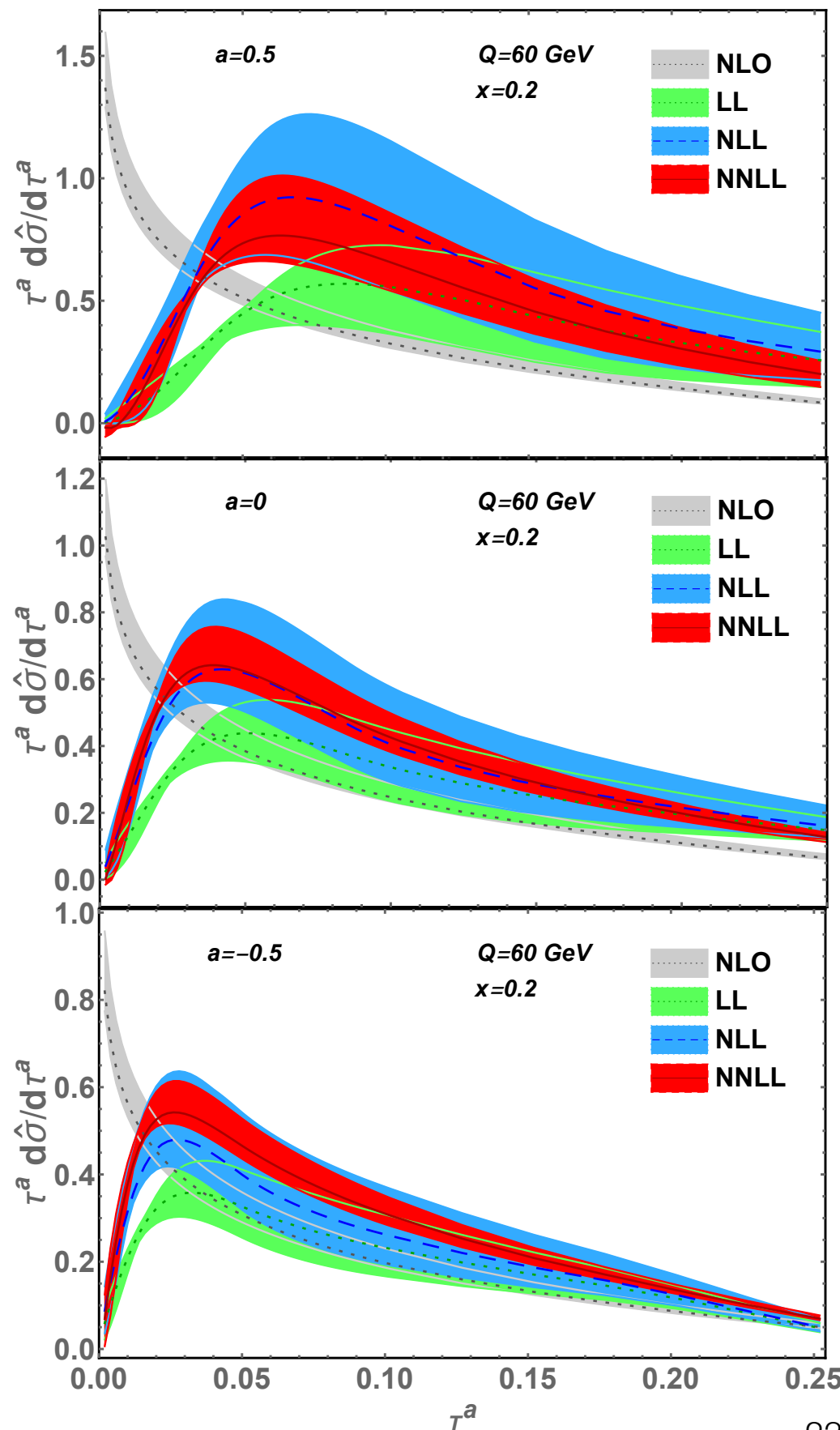
# Numerical results at NNLL

- DIS angularity cross-section at NNLL accuracy



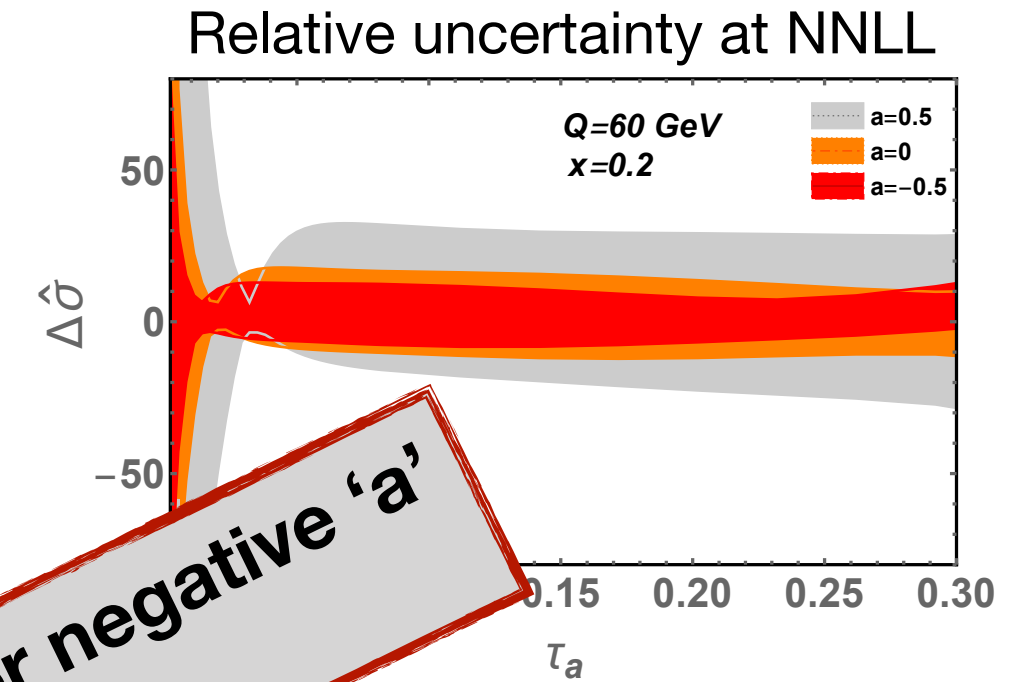
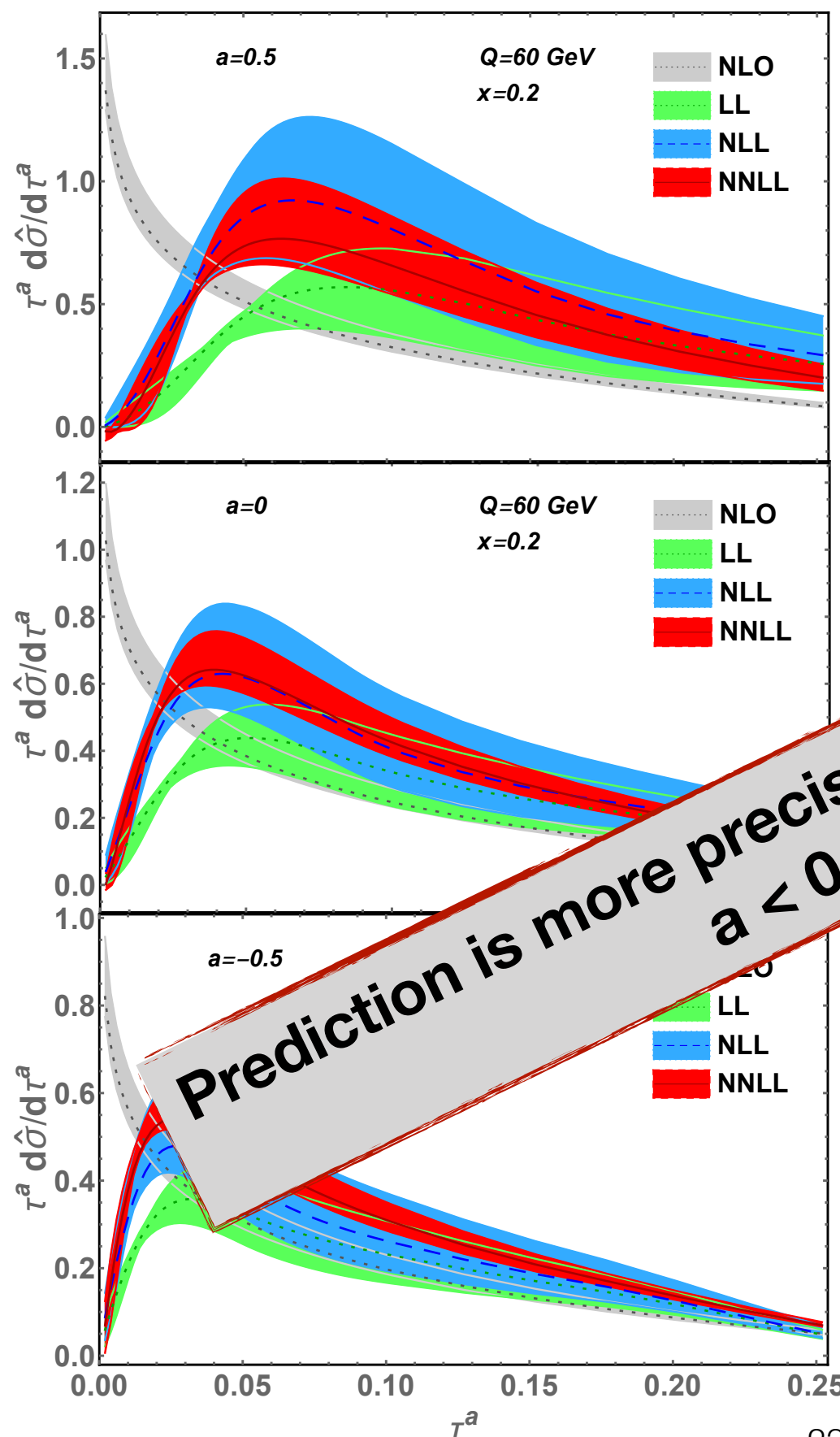
- We adopt electron-positron angularity profile function from Bell, Hornig, Lee, Talbert, 18

# 'a' dependency



📌 uncertainty in the DIS angularity cross-section depends on the angularity parameter 'a'

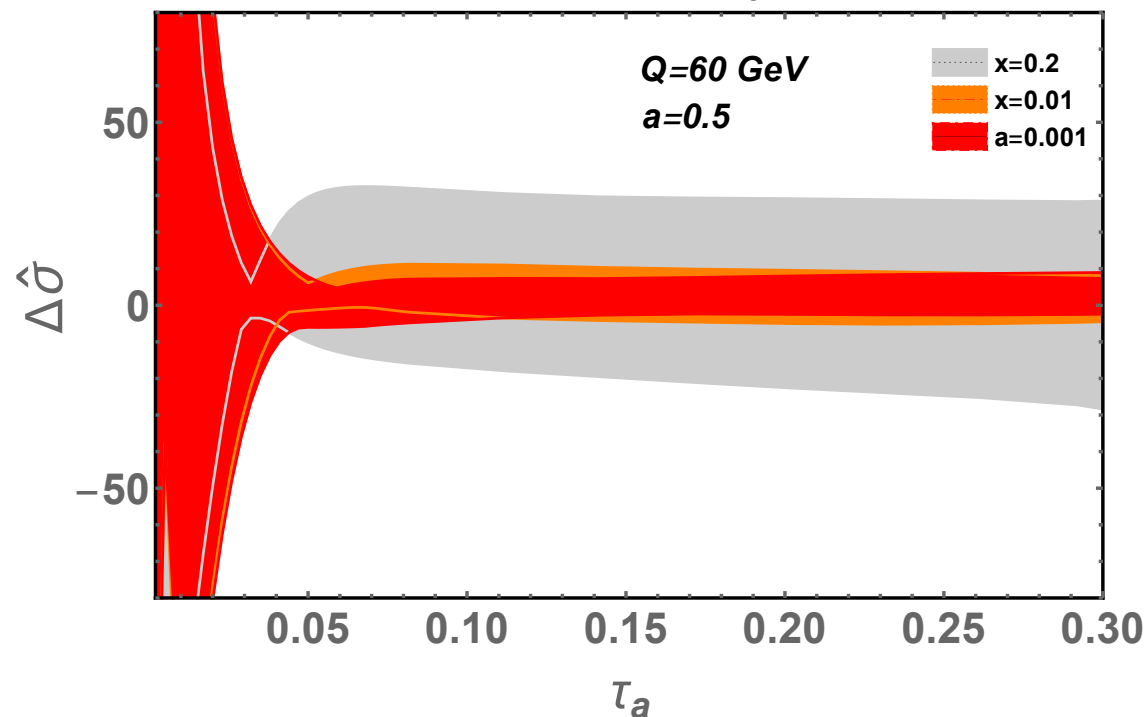
# 'a' dependency



📍 uncertainty in the DIS angularity cross-section depends on the angularity parameter 'a'

# 'x' dependency

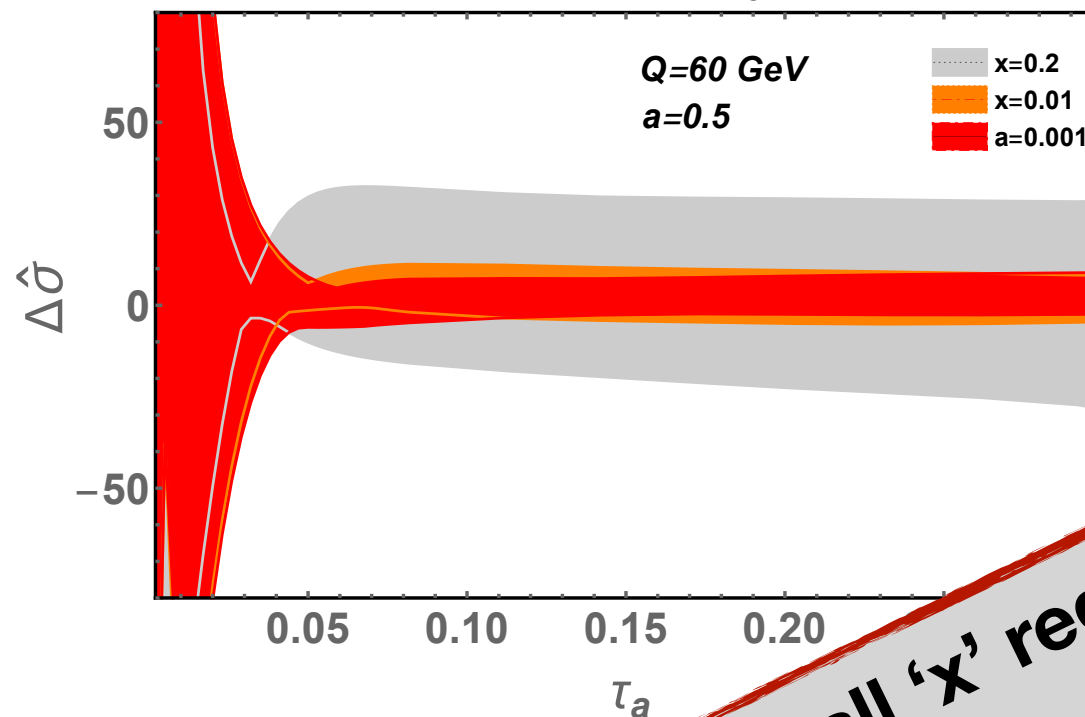
Relative uncertainty at NNLL



uncertainty in the angularity cross-section depends on the longitudinal momentum fraction (x) of the partons.

# 'x' dependency

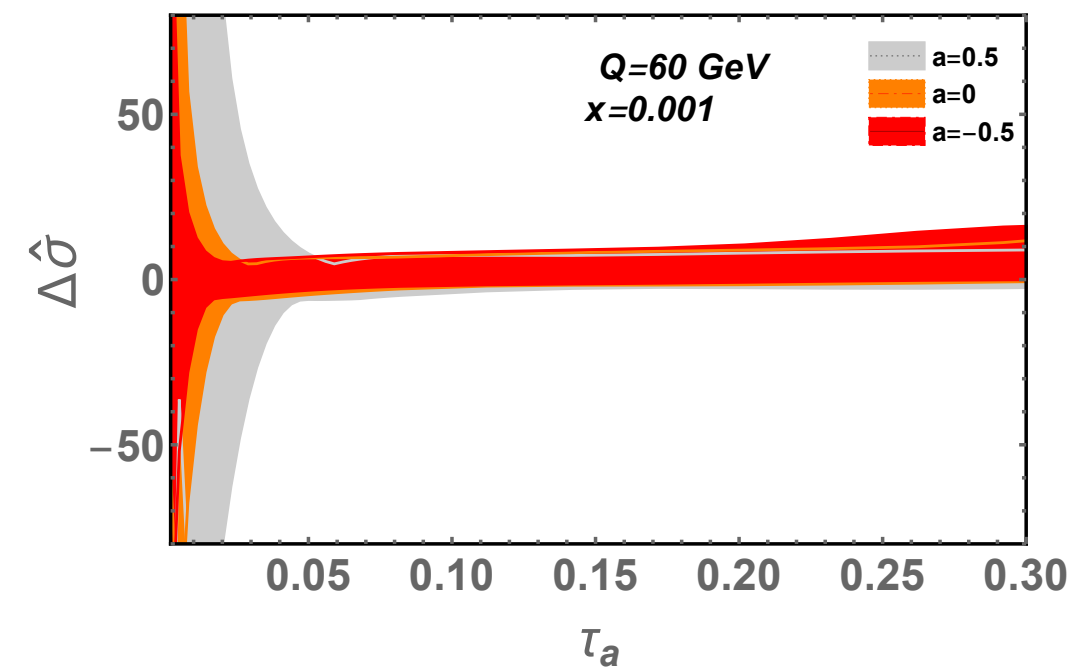
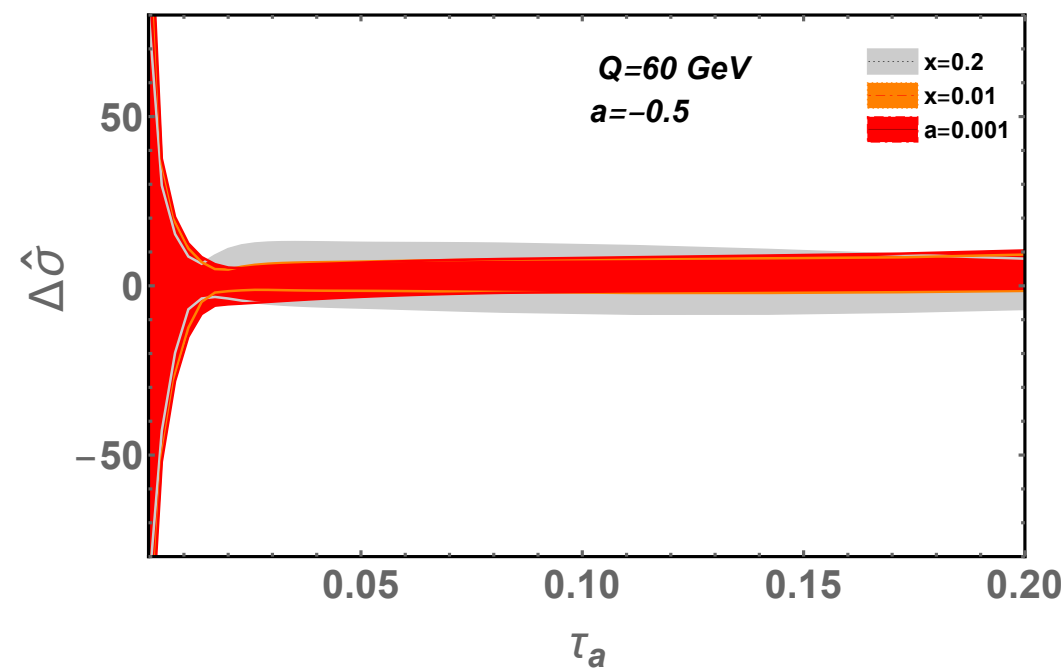
Relative uncertainty at NNLL



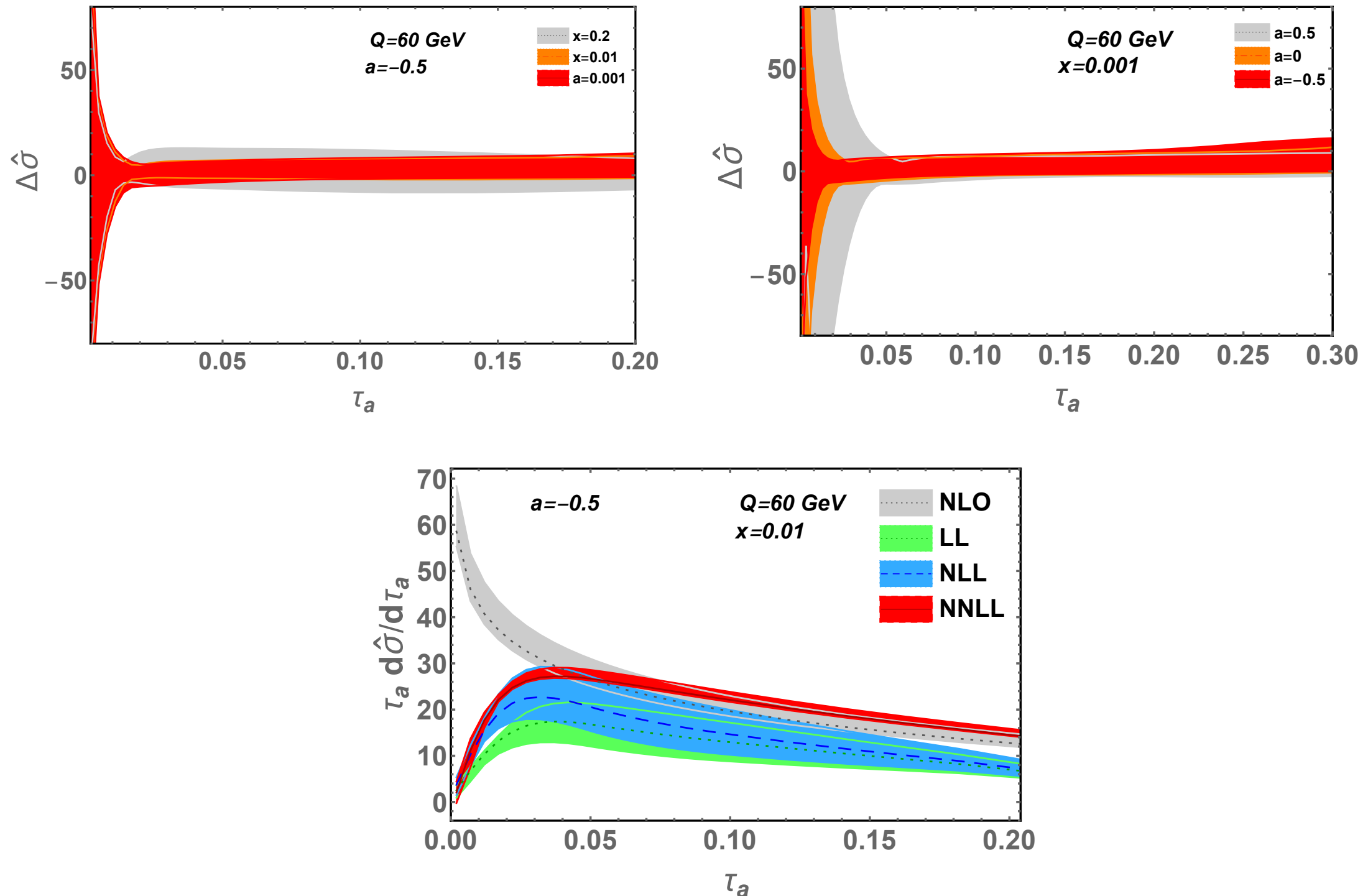
- uncertainty in the longitudinal section depends on the small-x interaction ( $x$ ) of the partons.

Prediction is more precise for small 'x' region.

## a < 0 and small-x result

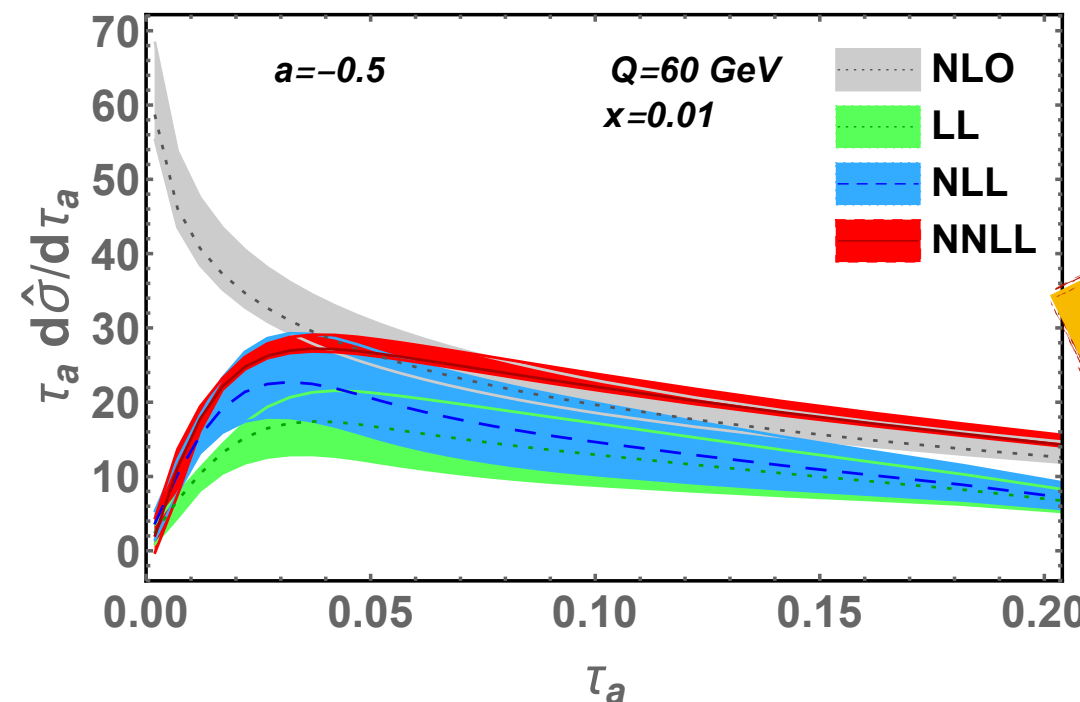
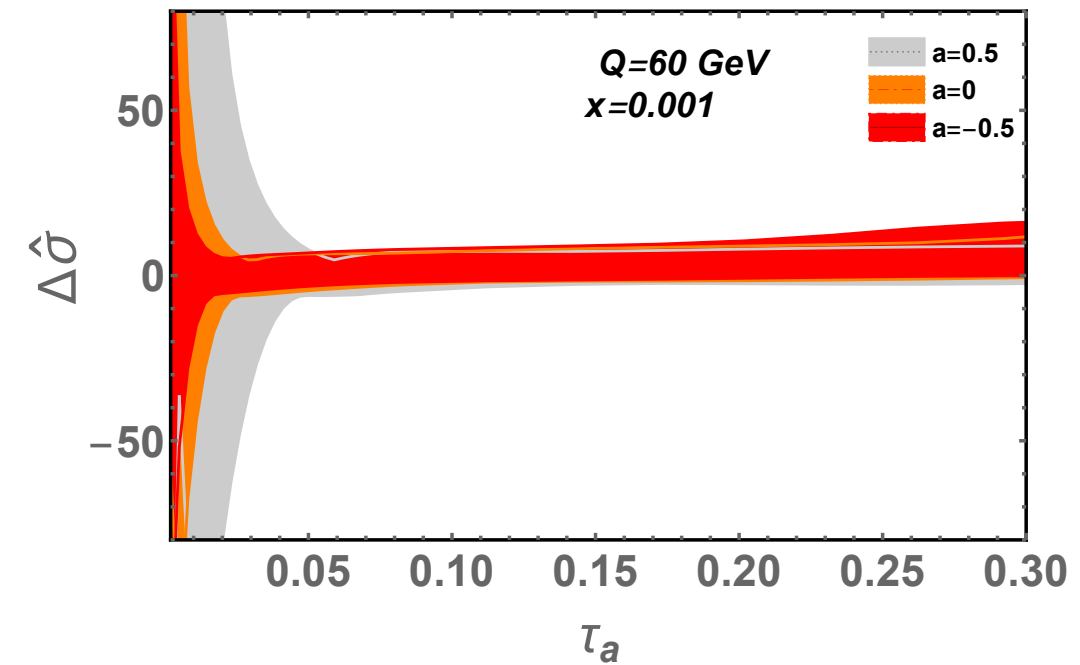
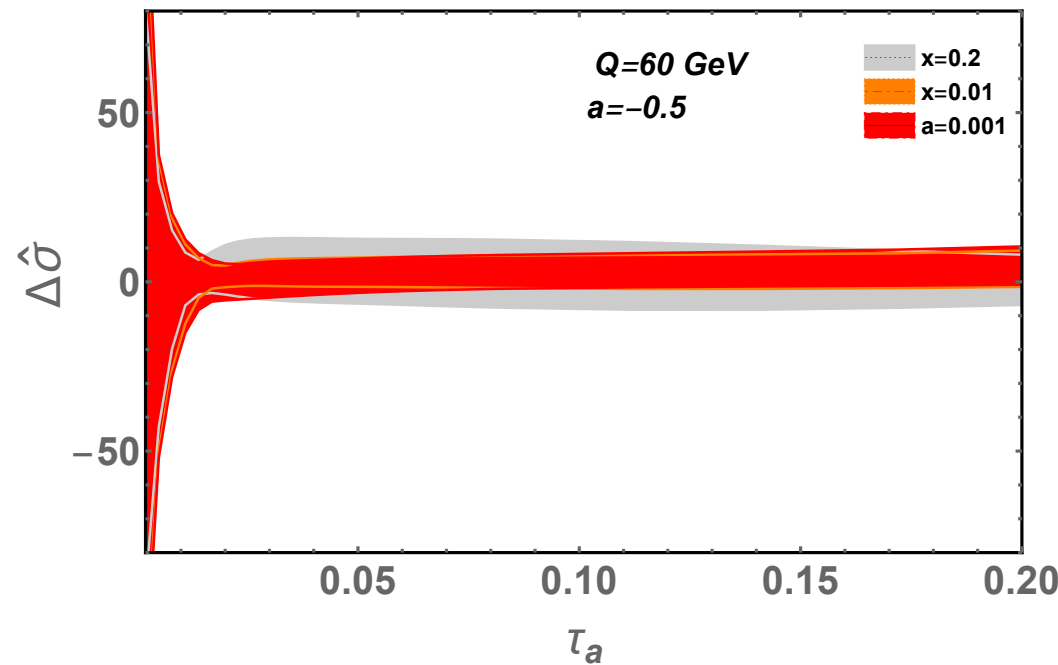


## a < 0 and small-x result



- Gluon contribution to the NLO correction is large at small- $x$  region

## a < 0 and small-x result



$a < 0$   
small-x region

- Gluon contribution to the NLO correction is large at small-x region

## Summary and Conclusion

---

1. Present one-loop angularity beam function for the axis choice along jet axis.
2. Give precision prediction to the DIS angularity cross-section at NNLL accuracy.

uncertainty depends on the angularity parameter ‘ $\alpha$ ’ as well as on the longitudinal momentum fraction ‘ $x$ ’ of the partons.

Prediction is more precise for small-‘ $x$ ’ and negative ‘ $\alpha$ ’ region.

## Future direction

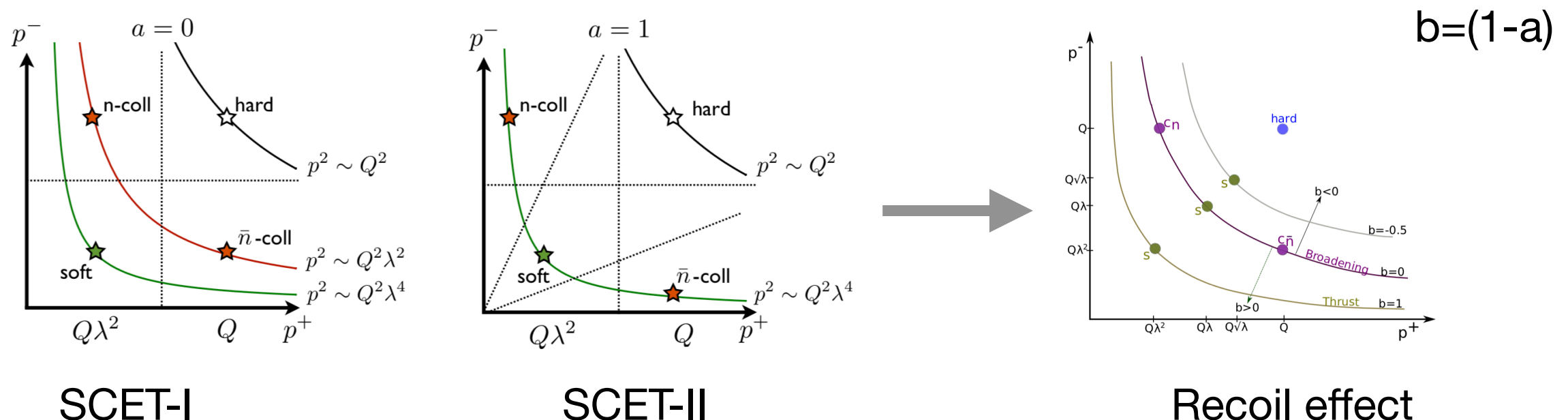
1. An extension of this work to access the entire  $a$  space, specially  $a \sim 1$  region, by incorporating the recoil effect.
2. Uncertainty in the cross-section is sensitive to  $Q$ , ' $a$ ' and 'x' and we need to find out a reasonable profile function for DIS angularity.



# Future direction

- 1. An extension of this work to access the entire  $a$  space, specially  $a \sim 1$  region, by incorporating the recoil effect.
  - 2. Uncertainty in the cross-section is sensitive to  $Q$ , ' $a$ ' and ' $x$ ' and we need to find out a reasonable profile function for DIS angularity.

1. Recoil effect in DIS angularity and access to the entire  $a$  space, specially  $a \sim 1$  region, by incorporating the recoil effect in DIS!!



- Andrew Hornig, Christopher Lee, and Grigory Ovanesyan, JHEP 05 (2009) 122
- A. Budhraja, Ambar Jain and Massimiliano Procura, JHEP08(2019)144



**Thank you!**



## Anomalous dimension

The universal cusp anomalous dimension  $\Gamma_{\text{cusp}}(\alpha_s)$  and non-cusp anomalous dimension  $\gamma_G(\alpha_s)$  are expressed in powers of  $\alpha_s$  as

$$\Gamma_{\text{cusp}}(\alpha_s) = \sum_{n=0} \Gamma_n \left( \frac{\alpha_s}{4\pi} \right)^{n+1}, \quad \gamma_G(\alpha_s) = \sum_{n=0} \gamma_n^G \left( \frac{\alpha_s}{4\pi} \right)^{n+1}, \quad (4.15)$$

where  $\Gamma_n$  are given in appendix D and one-loop result for  $\gamma_n^G$  are given in [36]

$$\gamma_0^G = \{-12C_F, 0, 6C_F\} \quad G = \{H, S, J\}, \quad (4.16)$$

which again satisfies the consistency in eq. (4.13) at the order  $\alpha_s$ . The two-loop hard anomalous dimension is well known [61, 63] and available up to three-loops [64]

$$\gamma_1^H = -2C_F \left[ \left( \frac{82}{9} - 52\zeta_3 \right) C_A + (3 - 4\pi^2 + 48\zeta_3) C_F + \left( \frac{65}{9} + \pi^2 \right) \beta_0 \right]. \quad (4.17)$$

$$\gamma_G(\mu) = j_G \kappa_G \Gamma_{\text{cusp}}(\alpha_s) L_G + \gamma_G(\alpha_s), \quad (4.11)$$

where  $\Gamma_{\text{cusp}}(\alpha_s)$  and  $\gamma_G(\alpha_s)$  are the cusp and non-cusp anomalous dimensions. The characteristic logarithm  $L_G$  is defined as

$$L_G = \begin{cases} \ln\left(\frac{Q}{\mu}\right) & G = H, \\ \ln\left[\frac{Q}{\mu}(\nu e^{\gamma_E})^{-1/j_G}\right] & G = \{\tilde{S}, \tilde{J}, \tilde{\mathcal{B}}\}, \end{cases} \quad (4.12)$$

The consistency relation followed by scale independence of cross section  $d\sigma(\mu)/d\mu = 0$  is given by  $\gamma_H(\mu) + \gamma_{\tilde{S}}(\mu) + 2\gamma_{\tilde{J}}(\mu) = 0$ , which is valid for any values of  $Q, \mu, \nu$  in eq. (4.11) and it turns into three consistency relations

$$\begin{aligned} j_H \kappa_H + j_S \kappa_S + 2j_J \kappa_J &= 0, \\ \kappa_S + 2\kappa_J &= 0, \\ \gamma_H(\alpha_s) + \gamma_S(\alpha_s) + 2\gamma_J(\alpha_s) &= 0. \end{aligned} \quad (4.13)$$

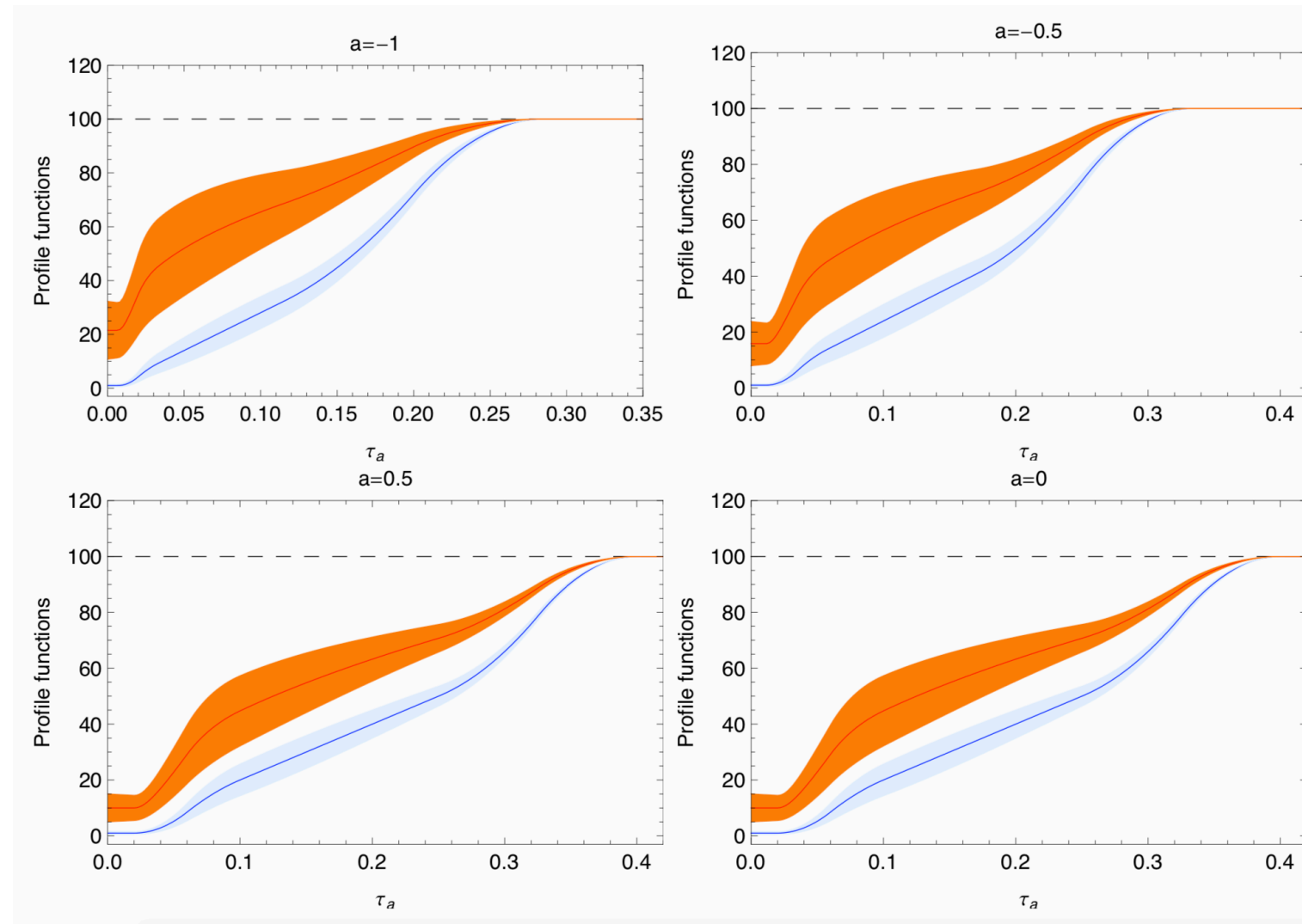
The constants  $j_G$  and  $\kappa_G$  are given by

$$\begin{aligned} j_G &= \{1, 1, 2-a\}, \\ \kappa_G &= \left\{4, \frac{4}{1-a}, -\frac{2}{1-a}\right\}, \quad G = \{H, S, J\} \end{aligned} \quad (4.14)$$

where  $C_{qj} = C_F, T_F$  for  $j = q, g$ . One of the logarithmic terms  $L_B$  is associated with PDF with the splitting functions  $P_{qj}$

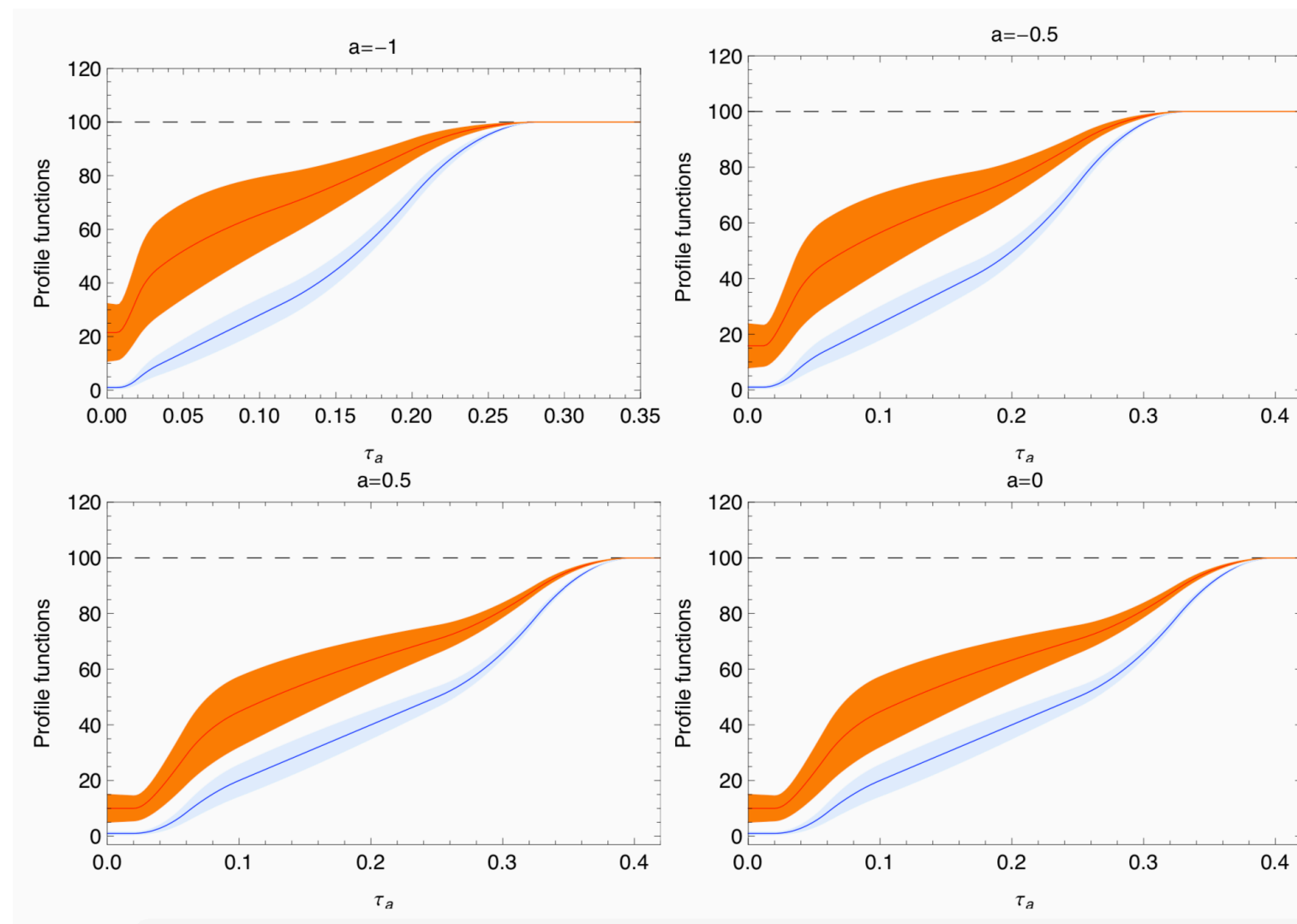
$$\begin{aligned} P_{qq}(z) &= \left[ \frac{\theta(1-z)}{1-z} \right]_+ (1+z^2) + \frac{3}{2} \delta(1-z) = \left[ \theta(1-z) \frac{1+z^2}{1-z} \right]_+, \\ P_{qg}(z) &= \theta(1-z)[(1-z)^2 + z^2]. \end{aligned} \quad (5.5)$$

# Profile function

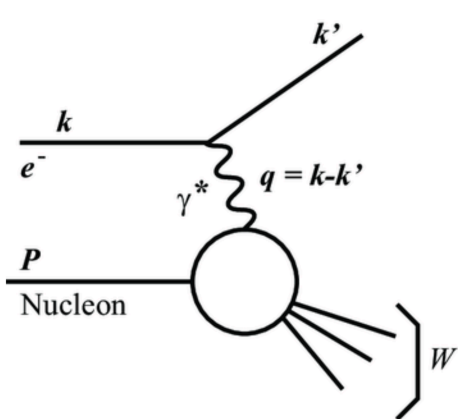


## Profile function

- We adopt electron-positron angularity profile function from Bell, Hornig, Lee, Talbert, 18



# DIS factorization in SCET



$$\frac{d\sigma}{dxdQ^2d\tau_a} = L_{\mu\nu}(x, Q^2) W^{\mu\nu}(x, Q^2, \tau_a)$$

The hadronic tensor defined by QCD current  $J^\mu(x) = \bar{\psi}\gamma^\mu\psi(x)$

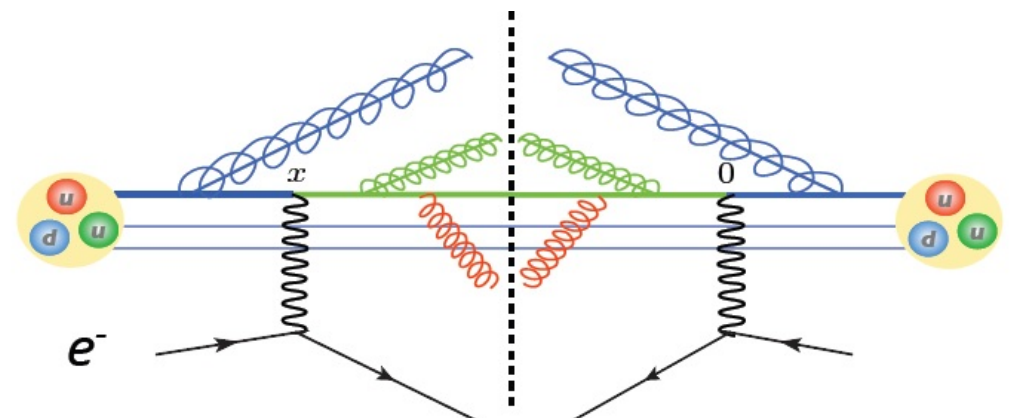
$$\begin{aligned} W^{\mu\nu}(x, Q^2, \tau_a) &= \sum_X \langle P | J^{\mu\dagger} | X \rangle \langle X | J^\nu | P \rangle (2\pi)^{(4)} \delta^4(P + q - p_X) \delta(\tau_a - \tau_a(X)) \\ &= \int d^4x e^{iq \cdot x} \langle P | J^{\mu\dagger}(x) \delta(\tau_a - \hat{\tau}_a) J^\nu(0) | P \rangle. \end{aligned}$$

Neglecting the power correction  $O(\lambda^2)$ , we match the current  $J^\mu(x) = \bar{\psi}\gamma^\mu\psi(x)$  onto the operators in SCET and perform the field redefinition to have factorized form of the hadronic tensor as

$$\begin{aligned} W_{\mu\nu}(x, Q^2, \tau_a) &= \left( \frac{8\pi}{n_J \cdot n_B} \right) \int d\tau_a^J d\tau_a^B d\tau_a^S \delta(\tau_a - \tau_a^J - \tau_a^B - \tau_a^S) \\ &\quad \times H_{\mu\nu}(q^2, \mu) \mathcal{B}_i(\tau_a^B, x, \mu) J(\tau_a^J, \mu) S(\tau_a^S, \mu) \end{aligned}$$

Measurement operator:  $\hat{\tau}_a = \hat{\tau}_a^{c_B} + \hat{\tau}_a^{c_J} + \hat{\tau}_a^S$

$$\begin{aligned} \frac{d\sigma}{dxdQ^2d\tau_a} &= \frac{d\sigma_0}{dxdQ^2} \int d\tau_a^J d\tau_a^B d\tau_a^S \delta(\tau_a - \tau_a^J - \tau_a^B - \tau_a^S) \\ &\quad \times \sum_{i=q,\bar{q}} H_i(Q^2, \mu) \mathcal{B}_i(\tau_a^B, x, \mu) J(\tau_a^J, \mu) S(\tau_a^S, \mu) \end{aligned}$$



**SCET facto.:**  $d\sigma = \text{Hard} \times \text{Beam} \otimes \text{Jet} \otimes \text{Soft}$

— D.Kang,Lee,Stewart'2013  
Z.Kang,Mantry,Qiu'2012